

5875 17.4 Solutions of Exercises of Chapter 9: Weak Focusing 5876 Synchrotron

5877 9.1 Construct SATURNE I. Spin Resonances

5878 A photo of SATURNE I synchrotron can be found in Fig. 9.1. A schematic layout
5879 of the ring and 90 deg cell is given in Fig. 9.22. This figure as well as Tab. 9.1
5880 which lists the parameters of the synchrotron, will be referred to in building the
5881 SATURNE I ring in the following.

5882 (a) A model of SATURNE I synchrotron.

5883 DIPOLE is used to simulate the 90° cell dipole, data are set for a hard-edge model
5884 in this exercise (for a DIPOLE model including fringe field, refer to the ZGS case,
5885 Exercise 9.2).

5886 It is necessary to have Fig. 17.55 at hand (in addition to the users' guide), when
5887 filling up the data list under DIPOLE. Some guidance regarding these data:

- 5888 • DIPOLE is defined in a cylindrical coordinate system.
- 5889 • AT is given the value of the bending sector extent: $AT=90$ degrees. The dipole
5890 EFBs coincide with DIPOLE entrance and exit boundaries.
- 5891 • RM is given the curvature radius value, $RM = B\rho/B = 0.274426548 \text{ [T m]}/$
5892 $0.03259493 \text{ [T]} = 8.4193 \text{ m}$, as it fits the geometry of the optical axis around the
5893 ring. The field value matches the reference rigidity under OBJET, these are the
5894 injection energy values, 3.6 MeV, proton.
- 5895 • $ACENT=45$ deg is the reference azimuth, for the positioning of the entrance and
5896 exit EFBs. It is taken half-way of the AT range, an arbitrary choice.

5897 $KPOS=2$ allows cancelling the coordinates of particle 1 (considered here as the
5898 reference trajectory, coinciding with the optical axis around the ring) at entrance
5899 and exit of DIPOLE:

- 5900 • The entrance and exit radii in and out of the AT sector for a particle on the closed
5901 orbit (*i.e.*, a particle travelling along the design optical axis) are $RE = RS = RM$.
- 5902 • The angle TE identifies with the closed orbit angle at the entrance boundary:
5903 $TE=0$, the closed orbit is normal to the EFB. TS identifies with the closed orbit
5904 angle at the exit boundary: $TE=0$, the closed orbit is normal to the EFB.

5905 A 90 deg sector in the hard edge model is given in Tab. 17.46; note that the
5906 sector has been split in two 45 deg halves, this is in order to allow a possible
5907 insertion of a beam monitor, so requiring $AT = 45$ deg, $\omega^+ = -\omega^- = 22.5$ deg.
5908 FAISCEAU located next to DIPOLE indicates that a trajectory entering DIPOLE
5909 at radius $R = RM$, normally to the EFB (thus, $Y_0 = 0$ and $T_0 = 0$ in OBJET) exits
5910 with $Y = 0$ and $T = 0$. Data validation at this stage can be performed by comparing
5911 DIPOLE's transport matrix computed with MATRIX (Tab. 17.47), and theoretical
5912 expectations (Sect. 15.2, Eq. 15.6):

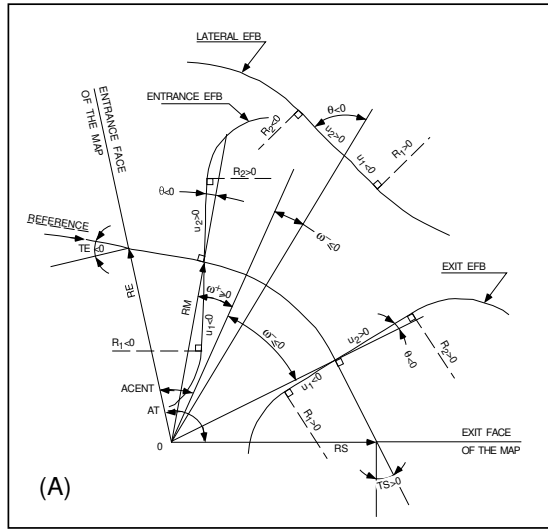


Fig. 17.55 A representation of the data that define a dipole magnet, using DIPOLE [1]

$$[T_{ij}] = \begin{pmatrix} 0.545794 & 11.15444 & 0 & 0 & 0 & 9.560222 \\ 0.062944 & 0.545794 & 0 & 0 & 0 & 1.324865 \\ 0 & 0 & 0.346711 & 10.19506 & 0 & 0 \\ 0 & 0 & -0.086295 & 0.346711 & 0 & 0 \\ 1.324865 & 9.560222 & 0 & 0 & 1 & 5.17640 \\ 0 & 0 & 0 & 0 & 0 & 1 \end{pmatrix} \quad (17.13)$$

5913

5914 Introducing fringe fields

5915 The SATURNE ring simulations which follow use the hard edge model. However, it
 5916 is leisable, at this point, to choose to add fringe fields in the model; here are the
 5917 changes which would be needed if so desired:

- 5918 • The bending sector is 90 degrees, however the field region extent AT has to
 5919 encompass the fringe fields, at both ends of the 90 deg sector. A 5 deg extension
 5920 is taken (namely, $ACENT - \omega^+ = AT - ACENT + \omega^- = 5 \text{ deg}$), for a total
 5921 $AT=100 \text{ deg}$ which allows $RM \times \tan(ACENT - \omega^+) \approx 74 \text{ cm}$; this large extension
 5922 ensures absence of truncation of the fringe fields at the AT sector boundaries,
 5923 over the all radial excursion of the beam.
- 5924 • $ACENT=50 \text{ deg}$ is the reference azimuth (an arbitrary value; taken half-way of
 5925 the AT range for convenience), for the positioning of the entrance and exit EFBs.
- 5926 • The entrance radius in the AT sector is $RE = RM / \cos(AT - \omega^+) = RM / \cos(5^\circ)$,
 5927 with $\omega^+ = 45 \text{ deg}$ the positioning of the entrance EFB with respect to $ACENT$.
 5928 And similarly for the positioning of the exit reference frame, $RS = RM / \cos(AT -$

Table 17.46 Simulation input data file: a pair of adjacent 45 degree sectors in the hard edge model. The magnet is split in order to allow insertion of FAISTORE or (here) FAISCEAU for beam monitoring. The reference optical axis has equal entrance (RE) and exit (RS) positions, and null angles (TE and TS), it coincides with the arc of radius $R = RM$ inside the sector. This input data file is named SatI_DIP.inc and defines the SATURNE I cell sequence segment S_SatI_DIP to E_SatI_DIP, for INCLUDE statements in subsequent exercises

```

File name: SatI_DIP.inc
! SATURNE I. Hard edge dipole model. Transport matrix.
'MARKER' SatI_DIP.inc_S ! Just for edition purposes.
'OBJET'
0.274426548e3 ! Reference Brho: 3.6 MeV proton.
5 ! Create a 13 particle set, proper for MATRIX computation.
.001 .01 .001 .01 .001 .0001 ! Coordinate sampling.
0. 0. 0. 0. 0. 1. ! Reference trajectory: all initial coordinates nul, relative rigidity D=1.
1
'MARKER' S_SatI_DIP ! Cell dipole begins here. A marker used for INCLUDEs in subsequent exercises.
'DIPOLE' upstream_half ! Analytical modeling of a dipole magnet.
0 ! set IL=2 here, to log trajectory coordinates in zgoubi.plt, at integration steps.
45. 841.93 ! Field region angle=90; reference radius set to curvature radius value.
22.5 0.3259493638 -0.6 0. 0. ! Reference angle ACENT set to AT/2; Bo field at RM; indices, all zero.
.0 0. ! EFB 1, hard-edged.
4 .1455 2.2670 -.6395 1.1558 0. 0. 0. ! Enge coefficients.
22.5 0. 1.E6 -1.E6 1.E6 1.E6 ! Angle to ACENT; face angle; face is straight.
.0 0. ! EFB 2, hard-edged.
4 .1455 2.2670 -.6395 1.1558 0. 0. 0.
-22.5 0. 1.E6 -1.E6 1.E6 1.E6 ! EFB 3. Unused.
0. 0.
0 0. 0. 0. 0. 0. 0. 0.
0 0. 1.E6 -1.E6 1.E6 1.E6 0.
2 1 ! Degree of interpolation polynomial; flying grid sizing.
2. ! Integration step size. It can be large in uniform field.
2 841.93 0. 841.93 0. ! Positioning of entrance and exit frames.
'MARKER' half-dipole !.plt ! Uncomment LABEL_2='!plt' (may go with IL=2 under DIPOLE) to
! log particle data in zgoubi.plt.
'FAISCEAU' ! Provides local coordinates, and ellipse parameters, at center of SATURNE I dipole.
'DIPOLE' downstream_half ! Analytical modeling of a dipole magnet.
0 ! set IL=2 here, to log trajectory coordinates in zgoubi.plt, at integration steps.
45. 841.93 ! Field region angle=90; reference radius set to curvature radius value.
22.5 0.3259493638 -0.6 0. 0. ! Reference angle ACENT set to AT/2; Bo field at RM; indices, all zero.
.0 0. ! EFB 1, hard-edged.
4 .1455 2.2670 -.6395 1.1558 0. 0. 0. ! Enge coefficients.
22.5 0. 1.E6 -1.E6 1.E6 1.E6 ! Angle to ACENT; face angle; face is straight.
.0 0. ! EFB 2, hard-edged.
4 .1455 2.2670 -.6395 1.1558 0. 0. 0.
-22.5 0. 1.E6 -1.E6 1.E6 1.E6 ! EFB 3. Unused.
0. 0.
0 0. 0. 0. 0. 0. 0. 0.
0 0. 1.E6 -1.E6 1.E6 1.E6 0.
2 1 ! Degree of interpolation polynomial; flying grid sizing.
2. ! Integration step size. It can be large in uniform field.
2 841.93 0. 841.93 0. ! Positioning of entrance and exit frames.
'MARKER' E_SatI_DIP ! Cell dipole ends here. A marker used for INCLUDEs in subsequent exercises.
'FAISCEAU' ! Local particle coordinates.
'MATRIX' ! Compute transport matrix, from trajectory coordinates.
1 0
'MARKER' SatI_DIP.inc_E ! Just for edition purposes.
'END'

```

- 5929 $(ACENT - \omega^-) = RM/\cos(5^\circ)$ with $\omega^- = -45$ deg the positioning of the exit
5930 EFB. Note that $\omega^+ - \omega^- = 90^\circ$, the value of the bend angle.
- 5931 • The entrance angle TE identifies with the angular increase of the sector: TE=5 deg.
5932 And similarly for the positioning of exit frame, 5 deg downstream of the exit EFB,
5933 thus TS=5 deg.
 - 5934 • Negative drifts with length $RM \times \tan(ACENT - \omega^+) = 0.7366545469$ cm need
5935 to be added upstream and downstream of DIPOLE, to account for the optical axis
5936 additional length over the 5 deg angular extent.

Table 17.47 Outcomes of the simulation file of Tab. 17.46

An excerpt from *zgoubi.res* execution listing. Coordinates of the first particle (considered here as the reference trajectory) and its path length under FAISCEAU, at OBJET on the left hand side below, locally on the right hand side:

```

3 Keyword, label(s) : FAISCEAU
                                TRACE DU FAISCEAU
                                (follows element # 2)
                                13 TRAJECTOIRES
                                OBJET
                                FAISCEAU
0 1 D Y(cm) T(mr) Z(cm) P(mr) S(cm) D-1 Y(cm) T(mr) Z(cm) P(mr) S(cm)
    1.0000 0.000 0.000 0.000 0.000 0.0000 0.0000 0.000 0.000 0.000 0.000 0.000 1.322501E+03

```

Transport matrix of SATURNE I 90 degree sector bend, in the hard edge model, two difference cases of integration step size, namely, 4 cm and 1 m (an excerpt of MATRIX computation, from *zgoubi.res* execution listing). It can be checked against matrix transport expectations. The “first order symplectic conditions” are very small in the 4 cm step size case, which is an indication of accurate numerical integration of the trajectories across DIPOLE; the reference trajectory (first one) exits better aligned (reference coordinates, before change of frame for MATRIX computation, are closer to zero):

- Case of 4 cm step size:

```

4 Keyword, label(s) : MATRIX
Reference, before change of frame (particle # 1 - D-1,Y,T,Z,s,time) :
0.00000000E+00 4.53054326E-07 6.27843350E-07 0.00000000E+00 0.00000000E+00 1.32250055E+03 4.41138700E-02

TRANSFER MATRIX ORDRE 1 (MKSA units)
0.545795 11.1544 0.00000 0.00000 0.00000 9.56022
-6.294423E-02 0.545795 0.00000 0.00000 0.00000 1.32487
0.00000 0.00000 0.346711 10.1951 0.00000 0.00000
0.00000 0.00000 -8.629576E-02 0.346711 0.00000 0.00000
1.32487 9.56022 0.00000 0.00000 1.00000 5.17640
0.00000 0.00000 0.00000 0.00000 0.00000 1.00000

DetY-1 = 0.0000000278, DetZ-1 = 0.0000000045

```

- Case of 1 m step size:

```

4 Keyword, label(s) : MATRIX
Reference, before change of frame (particle # 1 - D-1,Y,T,Z,s,time) :
0.00000000E+00 -7.54923113E-03 -1.08904867E-02 0.00000000E+00 0.00000000E+00 1.32249873E+03 4.41138091E-02

TRANSFER MATRIX ORDRE 1 (MKSA units)
0.545757 11.1567 0.00000 0.00000 0.00000 9.56154
-6.295274E-02 0.546125 0.00000 0.00000 0.00000 1.32517
0.00000 0.00000 0.346697 10.1954 0.00000 0.00000
0.00000 0.00000 -8.629900E-02 0.346750 0.00000 0.00000
1.32486 9.56148 0.00000 0.00000 1.00000 5.17692
0.00000 0.00000 0.00000 0.00000 0.00000 1.00000

DetY-1 = 0.0003978566, DetZ-1 = 0.0000685588

```

5937 (b) SATURNE I cell.

5938 A cell with origin in the middle of the drift is given Tab. 17.48, it is comprised of
5939 the split dipole and a pair of 2 m half-drifts at each ends (Fig. 9.22).

5940 *Closed orbit; chromatic closed orbit*

5941 The on-momentum closed orbit has been set to zero along the drifts ($Y_{c.o.} \equiv 0$),
5942 above, by a proper choice of RE, RS radii and TE, TS incidence angles.

Table 17.48 Simulation input data file: SATURNE I cell, assembled by INCLUDE-ing DIPOLE taken from Tab. 17.46 together with two half-drifts. This input data file is named SatI_cell.inc and defines the SATURNE I cell sequence segment S_SatI_cell to E_SatI_cell, for INCLUDE statements in subsequent exercises

```

File name: SatI_cell.inc.
! SATURNE I, one cell of the 4-period ring.
'MARKER' SatICellMATRIX_S ! Just for edition purposes.
'OBJET'
0.274426548e3 ! Reference Brho: 3.6 MeV proton.
5 ! Create a 13 particle set, proper for MATRIX computation.
.001 .01 .001 .01 .001 .0001 ! Coordinate sampling.
0. 0. 0. 0. 0. 1. ! Reference trajectory: all initial coordinates nul, relative rigidity D=1.

'MARKER' S_SatI_cell
'DRIFT' half_drift
200.
'INCLUDE'
1
./Sat_DIP.inc[S_SatI_DIP:E_SatI_DIP]
'DRIFT' half_drift
200.
'MARKER' E_SatI_cell
'FAISCEAU' ! Local particle coordinates.
'TWISS' ! Produce transport matrix, beam matrix, and periodic optical functions along the sequence.
2 1. 1.
'MARKER' SatICellMATRIX_E ! Just for edition purposes.
'END'

```

The radial coordinate of an off-momentum chromatic orbit can be estimated from the dispersion, Eq. 9.26, namely,

$$Y_{\delta} = \frac{\rho_0}{1-n} \frac{\delta p}{p} = 841.93 \frac{10^{-4}}{1-(-0.6)} \approx 0.21048 \text{ cm}$$

5943 whereas the orbit angle is zero, around the ring (on- and off-momentum closed orbits
5944 are parallel to the optical axis).

5945 Besides,

5946 - computation of an accurate value of Y_{δ} is performed adding FIT at the end of
5947 the cell;

5948 - in order to raytrace three particles, respectively on-momentum and at $\delta p/p =$
5949 $\pm 10^{-4}$, OBJET[KOBJ=2] is used;

5950 - in order to raytrace around the ring, for the purpose of plotting the closed orbit
5951 coordinates, a 4-cell sequence follows the FIT procedure.

5952 This results in the input data file given in Tab. 17.49. Running this input simulation
5953 file produces the following coordinates as per the FIT procedure (an excerpt from
5954 zgoubi.res execution listing):

```

5955 STATUS OF VARIABLES (Iteration # 4 / 999 max.)
5956 LMNT VAR PARAM MINIMUM INITIAL FINAL MAXIMUM STEP NAME LBL1 LBL2
5957 2 1 30 0.168 0.211 0.21056000 0.253 1.040E-05 OBJET - -
5958 2 2 40 0.00 0.00 0.00000000 0.00 0.00 OBJET - -
5959 2 3 50 -0.253 -0.210 -0.21040403 -0.168 1.040E-05 OBJET - -
5960 STATUS OF CONSTRAINTS (Target penalty = 1.0000E-10)
5961 TYPE I J LMNT# DESIRED WEIGHT REACHED KI2 NAME LBL1 LBL2 Nb param. [value]
5962 3 1 2 12 0.000000E+00 1.000E+00 1.466978E-06 6.70E-01 MARKER E_SatI_cell - - 0
5963 3 2 2 12 0.000000E+00 1.000E+00 6.028957E-07 1.13E-01 MARKER E_SatI_cell - - 0
5964 3 3 2 12 0.000000E+00 1.000E+00 8.357183E-07 2.17E-01 MARKER E_SatI_cell - - 0
5965 Fit reached penalty value 3.2139E-12

```

5966 The local coordinates Y , T and initial coordinates Y_0 , T_0 (as defined under OBJET)
5967 are identical to better than $5 \mu\text{m}$, $0.5 \mu\text{rad}$ accuracy, respectively, confirming the

5968 periodicity of these chromatic trajectories. Orbit coordinates around the ring are displayed in Fig. 17.56.

Table 17.49 Simulation input data file: first find the periodic orbit through a cell, then complete a 4-cell turn

```

SatI_Orbits.INC.dat: SATURNE I, on-momentum and chromatic orbits.
'MARKER' SatI_Orbits_S                               ! Just for edition purposes.
'OBJET'
0.274426548e3                                       ! Reference Brho: 3.6 MeV proton.
2                                                     ! Create particles individually.
3                                                     ! Three particles.
+.219560 0. 0. 0. 0. 1.0001 'p' ! Chromatic orbit coordinates Y0 and T0 for D=1.001 relative rigidity.
0. 0. 0. 0. 0. 1. 'o' ! On-momentum orbit.
-.210404 0. 0. 0. 0. 0.9999 'm' ! Chromatic orbit coordinates Y0 and T0 for D=0.999 relative rigidity.
1 1 1

'INCLUDE'
1
./SatI_cell.inc[S_SatI_cell:E_SatI_cell]

'FIT'
2
2 30 0 .2                                           ! Vary Y_0(particle 1) under OBJET.
2 50 0 .2                                           ! Vary Y_0(particle 3) under OBJET.
2
3.1 1 2 #End 0. 1. 0                               ! Constrain Y(particle 1)=Y_0(particle 1).
3.1 3 2 #End 0. 1. 0                               ! Constrain Y(particle 3)=Y_0(particle 1).

! When FIT is done converging on the constraints, execution quietly carries on with the periodic
! coordinates , raytracing through 4 cells to complete a turn around the ring.
'INCLUDE'
1
4 * ./SatI_cell.inc[S_SatI_cell:E_SatI_cell]

'SYSTEM'
1
gnuplot < gnuplot_Zplt_traj.gnu                       ! Plot the orbit radial coordiante.
'MARKER' SatI_Orbits_E                               ! Just for edition purposes.
'END'

```

A *gnuplot* script (excerpt) to obtain a graph of particle coordinates, from *zgoubi.plt* (as in Fig. 17.56):

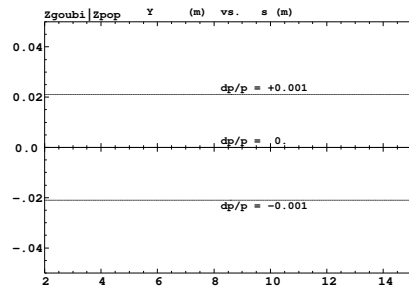
```

# gnuplot_Zplt_traj.gnu
traj1 = 1 ; traj2 = 3
plot \
for [i=traj1:traj2] 'zgoubi.plt' u ($19== i ? $14 *cm2m : 1/0):($10 *cm2m):($19) w p ps .4 lc palette

```

5969

Fig. 17.56 Radial coordinate of the orbits around the ring, on-momentum, and for $dp/p = \pm 10^{-3}$. A graph obtained using *zpop*, data read from *zgoubi.plt*: menu 7; 1/1 to open *zgoubi.plt*; 2/[6,2] for *Y* versus distance *s*; 7 to plot. A *gnuplot* script for a similar graph given is given in Tab. 17.49



5970 *Lattice parameters*

5971 The TWISS command down the sequence (Tab. 17.48) produces the periodic beam matrix results shown in Tab. 17.50; MATRIX[IFOC=11] would, as well. It also

Table 17.50 Results obtained running the simulation input data file of Tab. 17.48, SATURNE I cell - an excerpt from zgoubi.res execution listing

```

14 Keyword, label(s) : TWISS
Reference, before change of frame (particle # 1 - D-I,Y,T,Z,s,time) :
0.00000000E+00 6.02895730E-07 6.54169939E-07 0.00000000E+00 0.00000000E+00 1.72250055E+03 6.57784696E-01

Beam matrix (beta/-alpha/-alpha/gamma) and periodic dispersion (MKSA units)
14.418595 0.000000 0.000000 0.000000 0.000000 21.048250
0.000000 0.069355 0.000000 0.000000 0.000000 0.000000
0.000000 0.000000 11.411041 0.000000 0.000000 -0.000000
0.000000 0.000000 0.000000 0.087634 0.000000 0.000000
0.000000 0.000000 0.000000 0.000000 0.000000 0.000000
0.000000 0.000000 0.000000 0.000000 0.000000 0.000000

Betatron tunes (Q1 Q2 modes)
NU_Y = 0.18103144 NU_Z = 0.22214599

dL/L / dp/p = 1.9194487
(dp = 0.000000E+00 L(0) = 1.72250E+03 cm, L(0)-L(-dp) = 3.30606E-01 cm, L(0)-L(+dp) = -3.30645E-01 cm)

Transition gamma = 7.21791469E-01

Chromaticities :
dNu_y / dp/p = -0.60221729 dNu_z / dp/p = 0.38005442

```

5972

5973 produces a zgoubi.TWISS.out file which details the optical functions along the
5974 sequence (at the downstream end of the optical elements). The header of that file
5975 details the optical parameters of the structure (Tab. 17.51).

Table 17.51 An excerpt of zgoubi.TWISS.out file resulting from the execution of the SATURNE I cell simulation input data file of Tab. 17.48. Note that the ring (4-period) wave numbers are 4 times the cell values Q1, Q2 displayed here. Optical functions (betatron function and derivative, orbit, phase advance, etc.) along the optical sequence are listed as part of zgoubi.TWISS.out following the header. The top part and last line of that listing are given below

```

@ LENGTH      %le  17.22500552
@ ALFA        %le  1.919448707
@ ORBITS      %le  -0
@ GAMMATR    %le  0.7217914685
@ Q1          %le  0.1810314404 [fractional]
@ Q2          %le  0.2221459901 [fractional]
@ DQ1        %le  -0.6022172911
@ DQ2        %le  0.3800544183
@ DXMAX      %le  2.10586311E+01 @ DXMIN      %le  2.10482503E+01
@ DYMAY      %le  0.00000000E+00 @ DYMIN      %le  0.00000000E+00
@ XCOMAX     %le  2.10528899E-01 @ XCOMIN     %le  0.00000000E+00
@ YCOMAX     %le  0.00000000E+00 @ YCOMIN     %le  0.00000000E+00
@ BETXMAX    %le  1.57006971E+01 @ BETXMIN    %le  1.44132839E+01
@ BETYMAX    %le  1.30884296E+01 @ BETYMIN    %le  1.1411017E+01
@ XCORMS     %le  6.05227342E-04
@ YCORMS     %le  0. not computed
@ DXRMS      %le  2.98427468E-03
@ DYRMS      %le  0.00000000E+00

```

Optical functions listing zgoubi.TWISS.out (there is more: $D_{x,y}$, etc.: lines are truncated, here), including the periodic $\alpha_{x,y,1}$, $\beta_{x,y,1}$, $D_{x,y}$, etc.

```

# alfx      btx      alfy      bty      alfl      btl      Dx      Dxp
# 1         2         3         4         5         6         7         8
1.3683565E-08 1.4426805E+01 -6.6336606E-09 1.1411067E+01 0.0000000E+00 0.0000000E+00 2.1058631E+01 1.1261490E-03
2.3958789E-08 1.4426805E+01 -2.0952612E-10 1.1411067E+01 0.0000000E+00 0.0000000E+00 2.1048250E+01 3.4685148E-09
2.3958789E-08 1.4426805E+01 -2.0952612E-10 1.1411067E+01 0.0000000E+00 0.0000000E+00 2.1048250E+01 3.4685148E-09
-1.3863081E-01 1.4704066E+01 -1.7526845E-01 1.1761604E+01 0.0000000E+00 0.0000000E+00 2.1048250E+01 3.4685148E-09
-1.3863081E-01 1.4704066E+01 -1.7526845E-01 1.1761604E+01 0.0000000E+00 0.0000000E+00 2.1048250E+01 3.4685148E-09
5.1661104E-04 1.5700697E+01 2.2204071E-06 1.3088430E+01 0.0000000E+00 0.0000000E+00 2.1048250E+01 1.4621225E-09
5.1661104E-04 1.5700697E+01 2.2204071E-06 1.3088430E+01 0.0000000E+00 0.0000000E+00 2.1048250E+01 1.4621225E-09
1.3919474E-01 1.4692541E+01 1.7526999E-01 1.1761559E+01 0.0000000E+00 0.0000000E+00 2.1048250E+01 3.4685146E-09
1.3919474E-01 1.4692541E+01 1.7526999E-01 1.1761559E+01 0.0000000E+00 0.0000000E+00 2.1048250E+01 3.4685146E-09
4.3383067E-04 1.4413284E+01 7.7310157E-07 1.1411017E+01 0.0000000E+00 0.0000000E+00 2.1048250E+01 3.4685146E-09
4.3383067E-04 1.4413284E+01 7.7310157E-07 1.1411017E+01 0.0000000E+00 0.0000000E+00 2.1048250E+01 3.4685146E-09

```

5976 *Moving the origin of the cell*

5977 The origin of the sequence can be moved by placing both drifts on one side of
5978 DIPOLE. It can also be taken in the middle of DIPOLE, as the latter has been split.
5979 A fully deployed input data sequence (INCLUDEs accounted for) is provided at the
5980 top of the execution listing zgoubi.res, it can be used to copy-paste pieces around.
5981 It can then be checked that betatron tunes, chromaticities, momentum compaction
5982 (Tab. 17.50) do not change, and that the beam matrix does.

5983 *Optical functions along the cell*

They are computed by transporting the beam matrix, from the origin. A Fortran program available in zgoubi sourceforge package toolbox, betaFromPlt [1], performs this computation in the following way: OBJET[KOBJ=5.1] provides the initial beta function values (determined in the previous question); IL=2 under DIPOLE logs stepwise particle data in zgoubi.plt; 'split 10 2' added under DRIFT does it, too. The program betaFromPlt computes the transport matrix T_{step_i} from the origin of the sequence (at OBJET) to the considered step_i along the sequence, using particle

coordinates read in zgoubi.plt - a similar computation to what MATRIX does [1, MATRIX Sect.]. The beam matrix $\sigma = \begin{bmatrix} \beta & -\alpha \\ -\alpha & \gamma \end{bmatrix}$ is then transported, from the origin to step_i , using (Eq. 16.10)

$$\sigma_{\text{step}_i} = T_{\text{step}_i} \sigma_{\text{origin}} \tilde{T}_{\text{step}_i}$$

The result is displayed in Fig. 17.57.

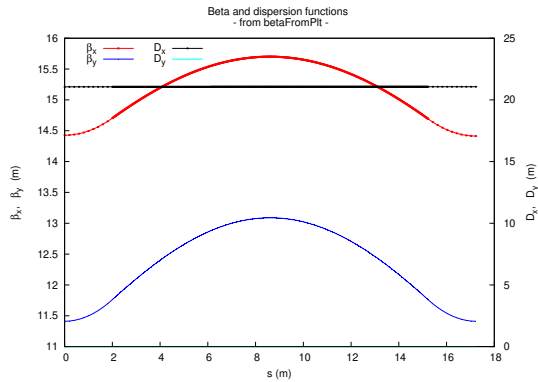


Fig. 17.57 Optical functions along SATURNE I cell. They are obtained from the transport of the beta functions, from the origin (at OBJET), using transport matrices computed from step-by-step particle coordinates stored in zgoubi.plt

5984

5985 *Tune scan*

5986 A simulation is given in Tab. 17.52, derived from Tab. 17.48: MATRIX[IFOC=11]
 5987 has been substituted to TWISS, a REBELOTE do loop repeatedly changes n . A
 5988 graph of the scan is given in Fig. 17.58, a few values are detailed in Tab. 17.53.

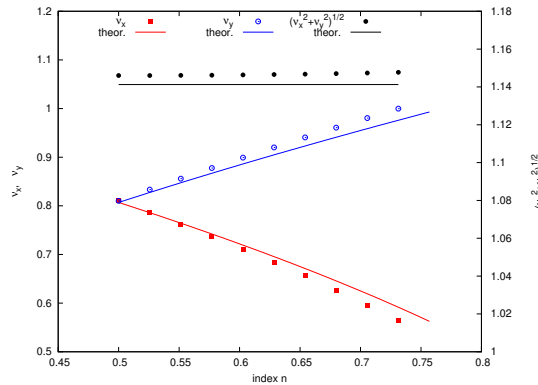


Fig. 17.58 A scan of the wave numbers, and of $\sqrt{v_Y^2 + v_Z^2} \approx \sqrt{R/\rho_0} = 1.141$, in SATURNE I for $0.5 \leq n \leq 0.757$. Solid curves are from theoretical approximations (Eq. 9.23), markers are from numerical simulations

Table 17.52 Simulation input data file: tune scan, using REBELOTE to repeatedly change n . Beam matrix and wave numbers are computed by MATRIX, from the coordinates of the 13 particle sample generated by OBJET[KOBJ=5]

```

SATURNE I, tune scan.
'MARKER' SatI_Qscan_S ! Just for edition purposes.
'OBJET'
0.274426548e3 ! Reference Brho: 3.6 MeV proton.
5 ! Create a 13 particle set, proper for MATRIX computation.
.001 .01 .001 .01 .001 .0001 ! Coordinate sampling.
0. 0. 0. 0. 0. 1. ! Reference trajectory: all initial coordinates nul, relative rigidity D=1.
1

'MARKER' S_SatI_cell
'DRIFT' half_drift
200.
'INCLUDE'
1
./SatI_DIP.inc[S_SatI_DIP:E_SatI_DIP]
'DRIFT' half_drift
200.
'MARKER' E_SatI_cell ! Local particle coordinates.
'FAISCEAU'
'MATRIX'
1 11 PRINT ! Comoute a 10+4 period transport matrix, and tunes. Save outcomes to zgoubi.MATRIX.out.

'REBELOTE' ! A do loop: repeat the section above commencing at the top of the file,
10 1.1 0 1 ! 10 times.
1
DIPOLE 6 -0.757:-0.5 ! Change the value of parameter 30 (namely, n) in DIPOLE (prior to repeating).
! in any DIPOLE in the sequence.

'SYSTEM'
1
gnuplot <./gnuplot_MATRIX_Qxy.gnu ! Plot tunes vs index.
'MARKER' SatI_Qscan_E ! Just for edition purposes.
'END'

```

gnuplot script to obtain Fig. 17.58:

```

# ./gnuplot_MATRIX_Qxy.gnu
set xlabel "index n";set ylabel "{/Symbol n}_x,    ({/Symbol n}_x^2+{/Symbol n}_y^2)^{1/2}"
set ylabel "{/Symbol n}_y"; set xtics; set ytics nomirror; set y2tics nomirror; ncell=4
set key t 1; set key maxrow 2; set yrange [:1.3]; set y2range [:1.06]
n1 = -0.757; dn=(.757-.5)/10.; R=10.9658; rho=8.4193
plot \
"zgoubi.MATRIX.out" u (n1+($61-1)*dn): \
($61>1? $56 *ncell :1/0) w p pt 5 lt 1 lw .5 lc rgb "red" tit "{/Symbol n}_x " ,\
"zgoubi.MATRIX.out" u (n1+($61-1)*dn):($61>1? sqrt((1+(n1+($61-1)*dn)*R/rho): \
1/0) w l lt 1 lc rgb "red" tit "theor. " ,\
"zgoubi.MATRIX.out" u (n1+($61-1)*dn): \
($61>1? $57 *ncell :1/0) axes xly2 w p pt 6 lt 3 lw .5 lc rgb "blue" tit "{/Symbol n}_y " ,\
"zgoubi.MATRIX.out" u (n1+($61-1)*dn): \
($61>1? sqrt((-n1+($61-1)*dn)*R/rho):1/0) axes x2y2 w l lt 3 lc rgb "blue" tit "theor. " ,\
"zgoubi.MATRIX.out" u (n1+($61-1)*dn): \
($61>1? sqrt($56**2+$57**2) *ncell :1/0) w p pt 7 lt 1 lc rgb "black" tit "({/Symbol n}_x^2+{/Symbol n}_y^2)^{1/2}" ,\
"zgoubi.MATRIX.out" u (n1+($61-1)*dn):($61>1? sqrt(R/rho):1/0) w l lt 1 lc rgb "black" tit "theor. "
pause 1

```

Table 17.53 Dependence of wave numbers on index n , from numerical raytracing (columns denoted “ray-tr.”) and from theory

n	v_Y		v_Z	
	ray-tr.	$\sqrt{(1-n)\frac{R}{\rho_0}}$	ray-tr.	$\sqrt{n\frac{R}{\rho_0}}$
0.5	0.810353	0.806987	0.810353	0.806987
0.6	0.724125	0.721791	0.888583	0.884010
0.7	0.626561	0.625089	0.960806	0.954840
0.757	0.563635	0.562580	0.999804	0.992955

The approximation

$$y(\theta) = A \cos(\nu_Z \theta + \phi)$$

5990 is checked here considering the vertical motion (considering the horizontal motion
5991 leads to similar conclusions). The value of the various parameters in that expression
5992 are determined as follows:

- the particle raytraced for comparison is launched with an initial excursion $Z_0(\theta = 0) = 5$ cm (4th particle in OBJET, above). At the launch point (middle of the drift) the beam ellipse is upright (Fig. 17.61), whereas phase space motion is clockwise, thus take

$$A = 5 \text{ cm} \quad \text{and} \quad \phi = \pi/2$$

- the vertical betatron of the 4-cell ring tune is (Tab. 17.51)

$$\nu_Z = 4 \times 0.222146 = 0.888284$$

- $\theta = s/R$ and $R = \oint ds/2\pi$ with (Tab. 17.51)

$$2\pi R = \text{circumference} = 2\pi \times 10.9658 = 68.9 \text{ m}$$

5993 The comparison with a trajectory obtained from raytracing is given in Fig. 17.59
5994 and confirms the validity of the sinusoidal approximation.

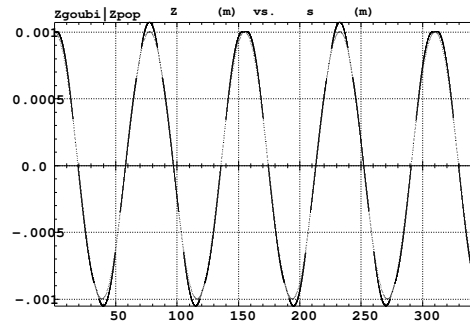


Fig. 17.59 Vertical betatron motion, five turns around SATURNE I ring, from raytracing (modulated oscillation), and sine approximation, superimposed

5995 (d) Beam envelopes.

5996 A few particles are launched through the cell with initial coordinates taken on a
5997 common invariant (horizontal and/or vertical), using OBJET[KOBJ=8]. The input
5998 data file is given in Tab. 17.54. The initial ellipse parameters (under OBJET) are
5999 the periodic values $\alpha_Y = \alpha_Z = 0$, $\beta_Y = 14.426$ m, $\beta_Z = 11.411$ m, found in
6000 zgoubi.TWISS.out (Tab. 17.51). The envelopes so generated, and the quantities
6001 $u^2(s)/\varepsilon_u/\pi$ (Eq. 9.22), are displayed in Fig. 17.60. The extremum extremorum
6002 value of $u^2(s)/\varepsilon_u/\pi$ comes out to be, respectively, $\hat{\beta}_Y = 14.4$ m and $\hat{\beta}_Z = 15.7$ m,
6003 consistent with earlier derivations (BETXMAX and BETYMAX values in Tab. 17.51
6004 and Fig. 17.57).

This raytracing also provides the coordinates of the particles on their common upright invariant (Fig. 17.61)

$$u^2/\beta_u + \beta_u u'^2 = \varepsilon_u/\pi$$

6005 at start and at the end of the cell ($\varepsilon_u/\pi = 10^{-4}$, here). This allows checking that the
 6006 initial ellipse parameters (under OBJET, Tab. 17.54) are effectively periodic values,
 6007 and that the raytracing went correctly, namely by observing that the initial and final
 6008 ellipses do superimpose.

Table 17.54 Simulation input data file: raytrace 60 particles across SATURNE I cell to generate beam envelopes. Store particle data in zgoubi.plt, along DRIFTS and DIPOLES. The INCLUDE file and segments are defined in Tab. 17.48

```

SATURNE I envelopes.
'MARKER' SatI_envelopes_S           ! Just for edition purposes.
'OBJET'
0.274426548e3                       ! Reference Brho: 3.6 MeV proton.
8                                     ! Create a set of 60 particles evenly distributed on the same invariant;
1 60 1   ! case of 60 particles on a vertical invariant; use 60 1 1 instead for horizontal invariant.
0. 0. 0. 0. 0. 1.
0. 14.426 1e-4
0. 11.411 1e-4
0. 1. 0.

'FAISTORE'                           ! This logs the coordinates of the particle to zgoubi.fai,
zgoubi.fai S_SatI_cell E_SatI_cell   ! at the two LABELIs as indicated.
1

'MARKER' S_SatI_cell                 ! SATURNE I cell begins here.
'DRIFT' half_Drift                   ! Option 'split' divides the drift in 10 pieces,
200. split 10 2                     ! 'IL=2' causes log of particle data to zgoubi.plt.

'INCLUDE'
1
./SatI_DIP.inc[S_SatI_DIP:E_SatI_DIP]

'DRIFT' half_Drift                   ! Option 'split' divides the drift in 10 pieces,
200. split 10 2                     ! 'IL=2' causes log of particle data to zgoubi.plt.

'MARKER' E_SatI_cell                 ! SATURNE I cell ends here.
'FAISCEAU'
'MARKER' SatI_envelopes_E           ! Just for edition purposes.
'END'

```

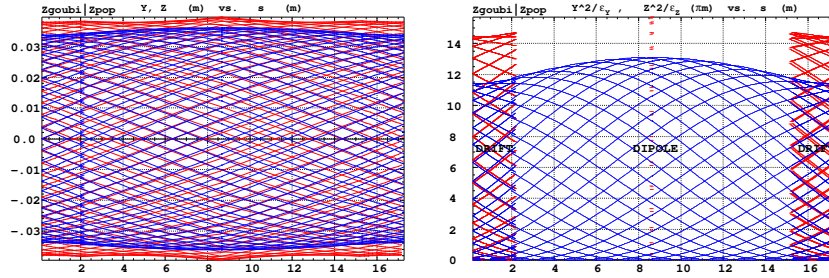


Fig. 17.60 Left: horizontal and vertical envelopes as generated by plotting the coordinates $Y(s)$ (greater excursion, red, along the drifts and dipole) or $Z(s)$ (smaller excursion, blue) across the SAT-URNE I cell, of 60 particles evenly distributed on a common $10^{-4} \pi$ m invariant, either horizontal or vertical (while the other invariant is zero). Right: a plot of $Y^2(s)/\epsilon_Y/\pi$ and $Z^2(s)/\epsilon_Z/\pi$; their extrema identify with $\beta_Y(s)$ and $\beta_Z(s)$, respectively. Graphs obtained using `zpop`, data read from `zgoubi.plt`: menu 7; 1/5 to open `zgoubi.fai`; 2/[6,2] (or [6,4]) for Y versus s (or Z versus s); 7 to plot; option 3/14 to raise Y (or Z) to the square

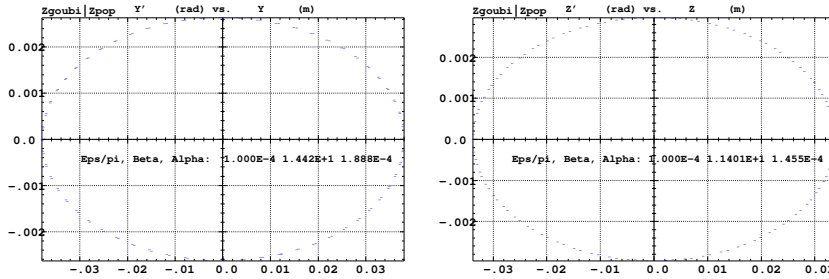


Fig. 17.61 Sixty particles evenly distributed on a common periodic invariant (either $\epsilon_Y = 10^{-4} \pi$ m and $\epsilon_Z = 0$, left graph, or the reverse, right graph) have been tracked through the cell. Initial and final phase space coordinates are displayed in these graphs: the initial and final ellipses which initial and final particle positions lie on superimpose. Optical function values given in the figures result from an *rms* match, of indifferently the initial or final coordinates; they do agree with the TWISS data (Tab.17.51). A graph obtained using `zpop`, data read from `zgoubi.fai`: menu 7; 1/5 to open `zgoubi.fai`; 2/[2,3] (or [4,5]) for T versus Y (or P versus Z); 7 to plot

6009 (e) An acceleration cycle. Symplecticity checks.

Eleven particles are launched for a 30,000 turn tracking at a rate of

$$\Delta W = q\hat{V} \cos \phi_s = 200 \times \sin 150^\circ = 100 \text{ keV/turn}$$

6010 ($E : 3.6 \rightarrow 3.0036 \text{ GeV}$), all evenly distributed on the same initial vertical invariant

$$Z^2/\beta_Z + \beta_Z Z'^2 = \epsilon_Z/\pi \tag{17.14}$$

6011 with $\epsilon_Z/\pi = 10^{-4} \text{ m}$, or, normalized, $\beta_Y \epsilon_Z/\pi = 0.08768 \times 10^{-4} \text{ m}$.

The simulation file is given in Tab. 17.55. `CAVITE[IOPT=3]` is used, it provides an RF phase independent boost

$$\Delta W = q\hat{V} \sin \phi_s$$

6012 as including synchrotron motion is not necessary here, even better, this ensures
 6013 constant depolarizing resonance crossing speed, so precluding any possibility of
 6014 multiple crossing (it can be referred to [3] regarding that effect).

Table 17.55 Simulation input data file: track 11 particles launched on the same vertical invariant. The INCLUDE adds the SATURNE I cell four times, the latter is defined in Tab. 17.48 and Fig. 9.22

```

SATURNE I ring. Polarization landscape.
'MARKER' SatIPolarLand_S ! Just for edition purposes.
'OBJET'
0.274426548e3 ! Reference Brho: 3.6 MeV proton.
8 ! Create a set of 60 particles evenly distributed on the same invariant;
1 11 1 ! case of 11 particles on a vertical invariant; use 11 1 1 instead for horizontal invariant.
0. 0. 0. 0. 0. 1.
0. 14.426 1e-4 ! Periodic optical functions and invariant value, horizontal and
0. 11.411 1e-4 ! vertical.
0. 1. 0. ! No momentum spread.

!'MCOBJET' ! Commented.
11.03527036749193e3 ! Reference Brho: 50 MeV proton.
13 ! Create a 13 particle set, proper for MATRIX computation.
!200
!2 2 2 2 2 2
!0. 0. 0. 0. 0. 1.
!0. 14.426 25e-6 3 ! Periodic alpha_Y, beta_Y, and invariant value;
!0. 11.411 10e-6 3 ! Periodic alpha_Z, beta_Z, and invariant value.
!0. 1. 1.e-8 3
!123456 234567 345678

'PARTICUL'
PROTON ! Necessary data in order to allow (i) spin trackingand, and (ii) acceleration.
'SPNTRK' ! Switch on spin tracking,
3 ! all initial spins vertical.
'FAISCEAU'
'FAISTORE'
b_polarLand.fai ! Log particle data in b_polarLand.fai, turn-by-turn; "b_" imposes
7 ! binary write, which results in faster i/o.

'SCALING'
1 1
DIPOLE
-1 ! Causes field increase in DIPOLE, in correlation to particle
1. ! rigidity increase by CAVITE.
1

! 4 cells follow.
'INCLUDE'
1
4* ./SatI_cell.inc[S_SatI_cell:E_SatI_cell]

'CAVITE'
3
0 0
200e3 0.523598775598 ! Acceleration rate is 200*0.5=100keV/turn.
! 20e3 0.523598775598 ! Commented: an acceleration rate of 20*0.5=10keV/turn.

'REBELOTE'
30000 0.2 99 ! Case of 100 keV/turn: ~30,000 turns from 3.6 MeV to 3 GeV.
! 300000 0.3 99 ! Commented: case of 10 keV/turn: ~300,000 turns from 3.6 MeV to 3 GeV.

'FAISCEAU'
'MARKER' SatIPolarLand_E ! Just for edition purposes.
'SPNPRT'

'END'

```

6015 *Betatron damping*

6016 Figure 17.62 shows the damped vertical motion of the individual particles, over
 6017 the acceleration range, together with the initial and final distributions of the 11
 6018 particles on elliptical invariants. Departure from the matching ellipse at the end of
 6019 the acceleration cycle, 3 GeV (Eq. 17.14 with $\epsilon_Z/\pi = 1.0745 \times 10^{-6}$ m), is marginal.

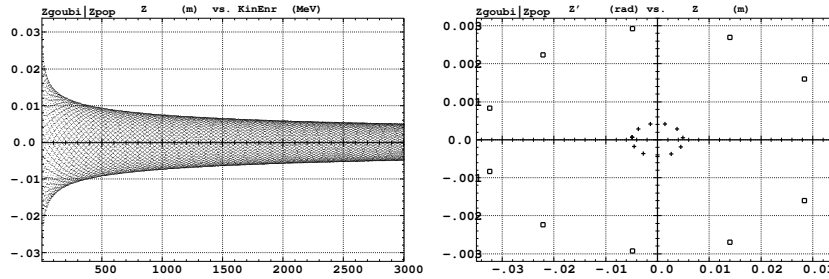
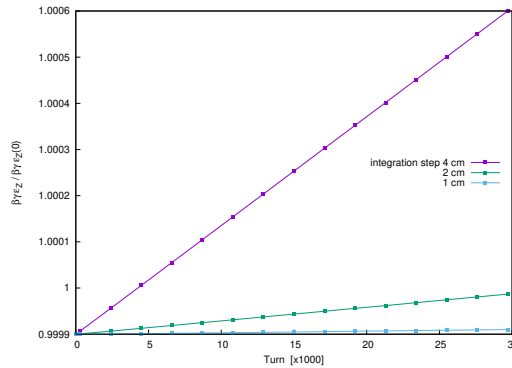


Fig. 17.62 Left: damped vertical motion, from 3.6 MeV to 3.004 GeV in 30,000 turns. Right: the initial coordinates of the 11 particles (squares) are taken on a common invariant $\epsilon_Z(0) = 10^{-4} \pi \text{m}$ (at 3.6 MeV, $\beta\gamma = 0.0877$, thus $\beta\gamma\epsilon_Z(0) = 8.77 \times 10^{-6} \pi \text{m}$); the final coordinates after 30,000 turns (crosses) appear to still be (with negligible departure) on a common invariant, of value $\epsilon_Z(\text{final}) = 2.149 \times 10^{-6} \pi \text{m}$ (at 3.004 GeV, $\beta\gamma = 4.08045$) or $\beta\gamma\epsilon_Z(\text{final}) = 8.77 \times 10^{-6} \pi \text{m}$, equal to the initial value $\beta\gamma\epsilon_Z(0)$

6020 *Degree of non-symplecticity of the numerical integration*

6021 The degree of non-symplecticity as a function of integration step size is illustrated
 6022 in Fig. 17.63. The initial motion is taken paraxial, vertical motion is considered as
 6023 it resorts to off-mid plane Taylor expansion of fields [1, DIPOLE Sect.], a stringent
 6024 test as the latter is expected to deteriorate further the non-symplecticity inherent
 6025 to the Lorentz equation integration method (a truncated Taylor series method [1,
 6026 Eq. 1.2.4]).

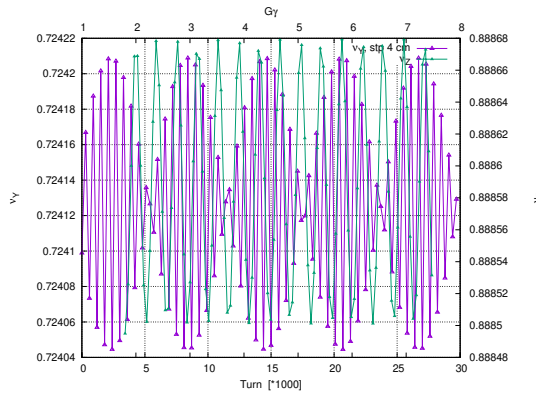
Fig. 17.63 Turn-by-turn evolution of the normalized invariant, $\beta\gamma\epsilon_Z(\text{turn})/\beta\gamma\epsilon_Z(0)$ (initial $\epsilon_Z(0)$ taken paraxial), for four different integration step size values: 1, 2 and 4 cm



6027 *Evolution of the wave numbers*

6028 The Fortran tool tunesFromFai_iterate can be used to computes tunes as a function of
 6029 turn number or energy, it reads turn-by-turn particle data from zgoubi.fai and
 6030 computes a discrete Fourier transform over so many turns (a few tens, 100 here
 6031 for instance), every so many turns (300, here) [4]. Typical results are displayed in
 6032 Fig. 17.64, tunes have the expected values: $\nu_Y = 0.7241$, $\nu_Z = 0.8885$. In acceleration
 6033 rate of 100 keV/turn has been taken (namely, $\hat{V} = 200$ kV and still $\phi_s = 150^\circ$), to
 6034 save on computing time. SCALING with option NTIM=-1 causes the magnet field
 6035 to strictly follow the momentum boost by CAVITE.

Fig. 17.64 Horizontal ring tune (left vertical axis), $\nu_Y \approx 0.7241$, and vertical ring tune (right vertical axis), $\nu_Z \approx 0.8885$, as a function of turn number, over 30,000 turns ($E : 0.0036 \rightarrow 3$ GeV at a rate of 100 keV/turn)



6036 (f) Crossing an isolated intrinsic depolarizing resonance.

6037 The simulation uses the input data file of Tab. 17.55, with the following changes:

- 6038 • Under OBJET:

- 6039 – 1st line, change the reference rigidity BORO for an initial $G\gamma \approx 2.95$, upstream
- 6040 of $G\gamma_R = 4 - \nu_Z \approx 3.1$,
- 6041 – 3rd line, request a single particle (“1 1 1”, in lieu of 11, “1 11 1”),
- 6042 – 6th line, set the invariant ε_Z/π to the desired value, ε_Y/π value is indifferent;
- 6043 resulting OBJET:

```

6044      'OBJET'
6045      4.08807740024e3          ! Reference Brho -> G*gamma=2.949312341 -> 605.22655 MeV proton.
6046      8                        ! Create a (set of) particle(s) on a given invariant.
6047      1 1 1                    ! case of 1 particle.
6048      0. 0. 0. 0. 0. 1.
6049      0. 1. 0.                  ! Horizontal invariant taken zero.
6050      0. 11.411 1e-4          ! Periodic alpha_Z, beta_Z, and invariant value.
6051      0. 1. 0.                ! No momentum spread.
    
```

- 6052 • change the field value under DIPOLE consistently with the new BORO value, so
- 6053 to maintain a curvature radius $\rho_0 = BORO/B = 8.4193$ m (Tab. 9.1),
- 6054 • under CAVITE, set the peak voltage to the required value,
- 6055 • under REBELOTE, set the number of turns to an appropriate value: a total of
- 6056 15,000, of which 8,000 about upstream of the resonance, is convenient for an
- 6057 acceleration rate of 10 keV/turn.

6058 *Changing the particle invariant value*

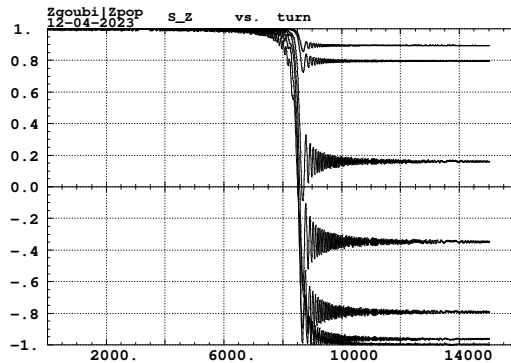
6059 Particle spin motion through the isolated resonance for seven different invariant

6060 values, $\varepsilon_Z/\pi = 1, 2, 10, 20, 40, 80, 200 \mu\text{m}$, observed at the beginning of the

6061 optical sequence (FAISTORE[b_polarLand.fai] location, Tab. 17.55), is displayed

6062 in Fig.17.65.

Fig. 17.65 Turn-by-turn spin motion through the isolated resonance $G\gamma_R = 4 - \nu_Z$, for 7 different values of the particle invariant from (top to bottom) $1 \mu\text{m}$ to $200 \mu\text{m}$ where full spin flip occurs. A graph obtained using zpop, data read from b_polarLand.fai: menu 7; 1/8 to open b_polarLand.fai; 2/[39,23] for S_Z versus turn; 7 to plot



6063 The intrinsic resonance strength satisfies $|\epsilon_R|^2 = A \varepsilon_Z$, with A a factor which char-

6064 acterizes the lattice. On the other hand, from the Froissart-Stora formula (Eq. 9.39)

6065 one gets

$$|\epsilon_R|^2 = \frac{2\alpha}{\pi} \ln \left(\frac{2}{1 + S_{Z,f}/S_{Z,i}} \right) \xrightarrow{S_{Z,f} \approx S_{Z,i}} \frac{\alpha}{\pi} \left(1 - \frac{S_{Z,f}}{S_{Z,i}} \right) \quad (17.15)$$

6066 with α , crossing speed, a constant. Thus one expects to find $\frac{1}{\varepsilon_Z} \ln \left(\frac{2}{1+S_{Z,f}/S_{Z,i}} \right)$ con-
 6067 stant. This property is not strictly satisfied by the tracking outcomes, Tab. 17.56,
 6068 explain why.

6069 Calculation of the resonance strength from the P_f/P_i tracking results, using
 6070 Eq. 17.15, requires the value of the crossing speed, which is

$$\alpha = \frac{1}{2\pi} \frac{\Delta E}{M} = \frac{1}{2\pi} \frac{20 \times 10^3 \times \sin 30^\circ \text{ [eV/turn]}}{938.27208 \times 10^6 \text{ [eV]}} = 1.696 \times 10^{-6} \quad (17.16)$$

6071 Table 17.56, rightmost column, displays the ratio $|\epsilon_R|^2/\varepsilon_Z/\pi$ so obtained, essentially
 constant as expected.

Table 17.56 Relationship between the invariant value ε_Z/π and the quantity $\ln \left(\frac{2}{1+S_{Z,f}/S_{Z,i}} \right) \propto$
 $|\epsilon_R|^2$ (Eq. 17.15). $\hat{V} = 20$ kV, here, crossing speed $\alpha = 1.696 \times 10^{-6}$ (Eq. 17.16). $S_{Z,i} = 1$ always,
 and $S_{Z,f}$ (col. 2) is a rough estimate from Fig. 17.65. The rightmost column gives the resulting ratio
 $|\epsilon_R|^2/\varepsilon_Z/\pi$, essentially constant

ε_Z/π (μm)	$\frac{S_{Z,f}}{S_{Z,i}} \equiv S_{Z,f}$	$\ln \frac{2}{1+S_{Z,f}}$	$\frac{ \epsilon_R ^2}{\varepsilon_Z/\pi}$ ($\times 10^{-8}$)
1	0.89	0.024568	2.652645
2	0.795	0.046965	2.535451
10	0.17	0.232844	2.514034
20	-0.35	0.488116	2.635115
40	-0.78	0.958607	2.587537
80	-0.975	1.903089	2.568474

6072

6073 *Changing the crossing speed*

6074 The crossing speed is reduced by a factor of 2, using $\hat{V} = 10$ kV, and accordingly
 6075 the number of turns is doubled, to 30,000, the only modifications to the input data
 6076 simulation file used in the previous question. Tracking results, Tab. 17.57, show that
 6077 $\frac{\hat{V}}{\varepsilon_Z/\pi} \times \ln \left(\frac{2}{1+S_{Z,f}/S_{Z,i}} \right)$ is constant, as expected.

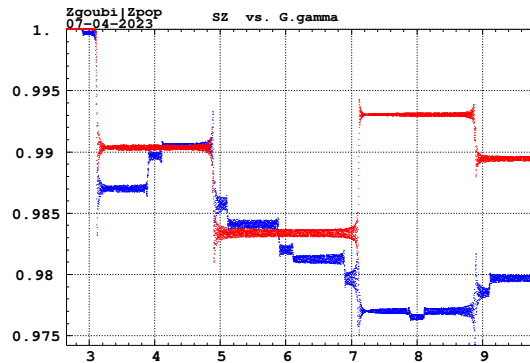
Table 17.57 Relationship between the acceleration rate $\Delta E \propto \hat{V}$ and the quantity $\ln\left(\frac{2}{1+S_{Z,i}/S_{Z,i}}\right)$. Normalized to ε_Z/π , their product (rightmost column) appears to be essentially constant, this is the expected result

ε_Z/π (μm)	\hat{V} (kV)	$\frac{S_{Z,i}}{S_{Z,i}} \equiv S_{Z,i}$	$\ln \frac{2}{1+S_{Z,i}}$	$\frac{\hat{V}}{\varepsilon_Z/\pi} \times \ln \frac{2}{1+S_{Z,i}}$
1	10	+0.79	0.048	0.482
10	10	-0.33	0.475	0.475
20	10	-0.78	0.959	0.479
1	20	+0.89	0.025	0.49
2	20	+0.795	0.047	0.47

6078 *Systematic resonances, random resonances*

6079 A single-particle tracking is pushed beyond $G\gamma = 8 + \nu_Z \approx 8.89$, 40,000 turns at
 6080 a rate of 100 kV/turn. The resulting $S_Z(G\gamma)$, Fig. 17.66, shows that in a 4-periodic
 6081 lattice the sole systematic resonances are excited, whereas all resonances are excited
 6082 if the 4-periodicity is broken - here, by changing the index to $n = -0.66$ in one
 DIPOLE, the periodicity is 1.

Fig. 17.66 Resonance crossing in SATURNEI, a turn-by-turn record of $S_Z(G\gamma)$. Case of systematic resonances $G\gamma = 4k \pm \nu_Z$ in a 4-period lattice (red), and of random resonances $G\gamma = k \pm \nu_Z$ in a 1-periodic perturbed optics lattice (blue). A graph obtained using zpop, data read from b_polarLand.fai: menu 7; 1/8 to open b_polarLand.fai; 2/[59,23] for S_Z versus $G\gamma$; 7 to plot



6083

6084 (g) Spin motion across a weak depolarizing resonance.

6085 The goal is to check numerical outcomes against the Fresnel integral model
 6086 (Eq. 9.41). A weak resonance is obtained using small amplitude vertical motion and
 6087 fast crossing.

6088 A single particle is raytraced, in the following conditions:

- 6089 - resonance to be crossed: $G\gamma_R = 4 - \nu_y \approx 3.1115$,
- 6090 - acceleration: peak voltage $\hat{V} = 100$ kV, synchronous phase $\phi_s = 30^\circ$,
- 6091 - particle invariant $\varepsilon_Z/\pi = 10^{-6}$ m.

6092 The initial rigidity is taken a few hundred turns upstream of the resonance, namely,
 6093 $B\rho_{\text{ref}} = 4.0880774$ T m, 605226550 MeV, $G\gamma = 2.94931241$, a distance to $G\gamma_R$ of

6094 $4 - \nu_Z - 2.949312415 \approx 0.16223$. Tracking extends a few thousand turns beyond
 6095 $G\gamma_R$ so that S_Z reaches its asymptotic value, from which the resonance strength $|\epsilon_R|$
 6096 can be calculated, using Eq. 17.15.

6097 The simulation file is given in Tab. 17.58. Note the new setting of the SCALING
 6098 factor SCL: DIPOLE field was set for a curvature radius $\rho_0 = 8.4193$ m, given a
 6099 reference rigidity $B\rho_{\text{ref}} \equiv BORO = 0.274426548$ Tm (Tab. 17.46). However the
 6100 reference rigidity is now changed to $B\rho_{\text{ref}} = 4.0880774$ Tm, thus maintaining ρ_0
 6101 requires scaling the field in DIPOLE by $4.0880774/0.274426548 = 14.8968$ at turn
 6102 1: this is the new factor, $SCL = 14.8968$, under SCALING (Tab. 17.58). Option
 6103 NT=-1 under SCALING ensures that the scaling factor will automatically follow,
 6104 turn-by-turn, the rigidity boost by CAVITE so preserving constant curvature radius
 6105 $\rho_0 = 8.4193$ m.

6106 The resulting turn-by-turn spin motion is displayed in Fig. 17.67. The Fresnel
 6107 integral model (Eq. 9.41) has been superimposed. Parameters in the latter are as
 6108 follows:

- 6109 - crossing speed $\alpha = \frac{1}{2\pi} \frac{\Delta E}{M} = \frac{1}{2\pi} \frac{10^5 \times \sin 30^\circ [\text{eV/turn}]}{938.27208 \times 10^6 [\text{eV}]} = 8.4812 \times 10^{-6}$,
 - asymptotic $S_{Z,f} = 0.999780$, whereas initial $S_{Z,i} = 1$, thus (Eq. 17.15)

$$|\epsilon_R|^2 = 5.939 \times 10^{-10}$$

6110 - orbital angle origin set at the location of $G\gamma_R$, which is turn 1699.

Fig. 17.67 Turn-by-turn spin motion through the isolated resonance $G\gamma_R = 4 - \nu_Z$, case of weak resonance strength. Modulated curve (blue): from raytracing. Smooth curve (black): Fresnel integral model

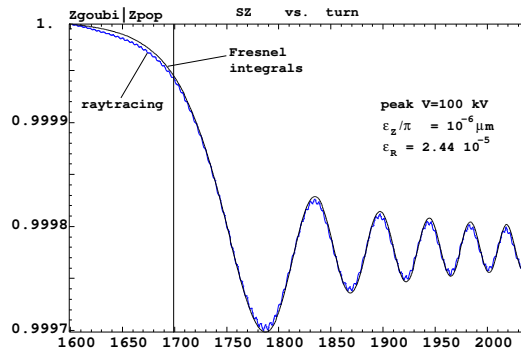


Table 17.58 Simulation input data file: track a particle launched on a vertical invariant $\varepsilon_y/\pi = 10^{-6}$ m, with horizontal motion indifferent, taken zero here. The INCLUDE adds the SATURNE I cell four times, the latter is defined in Tab. 17.48 and Fig. 9.22

```

SATURNE I ring. Crossing Ggamma=4-nu_Z, weak resonance case (small vertical invariant)
'MARKER' SatIWeakXing_S ! Just for edition purposes.
'OBJET'
4.08807740024e3 ! Reference Brho: 605226550 MeV proton.
8 ! Create a (set of) particle(s) on a given invariant.
1 1 1 ! create a single particle.
0. 0. 0. 0. 0. 1.
0. 14.426 0 ! Horizontal invariant is null.
0. 11.411 1e-6 ! Periodic alpha_Z, beta_Z, and invariant value.
0. 1. 0. ! No momentum spread.
'PARTICUL'
PROTON ! Necessary data in order to allow (i) spin trackingand, and (ii) acceleration.
'SPNTRK' ! Switch on spin tracking.
3 ! nitial spin vertical.
'FAISCEAU'
'FAISTORE'
xing4-Qy.fai ! Log particle data in xing.fai, turn-by-turn.
1

'SCALING'
1 1
DIPOLE
-1 ! Causes field increase in DIPOLE to follow rigidity increase by CAVITE.
14.8968 ! Relative rigidities at turn 1.
1

! 4 cells follow.
'INCLUDE'
1
4* ./SatI_cell.inc[S_SatI_cell:E_SatI_cell]

'CAVITE'
3
0 0
200e3 0.523598775598 ! Acceleration rate is 200*0.5=100keV/turn.

'REBELOTE'
3999 0.3 99 ! A total of 3999+1=4000 turns.

'FAISCEAU'
'MARKER' SatIWeakXing_E ! Just for edition purposes.
'SPNPRT'

'END'

```

6111 (h) Stationary spin motion near a resonance

6112 The simulation input data file of Tab. 17.58 can be used for these fixed energy
6113 trials, with some changes, as follows:

6114 - OBJET[KOBJ=1] is used as it allows to define a set of particles with sampled
6115 momentum offset, namely:

```

6116 'OBJET'
6117 4.4393621786553803e3 ! BORO taken as close to resonant G.gamma as prior knowledge of nu_Z allows.
6118 1 ! Create a set of particles.
6119 1 1 1 1 1 41 ! 41 particles sampling a
6120 0. 0. 0. 0. 0. .00001 ! momentum offset, in -20*1e-5< D-1 < 20*1e-5.
6121 0. 0. 3. 0. 0. 1. ! All particles have initial Z=3cm.
6122

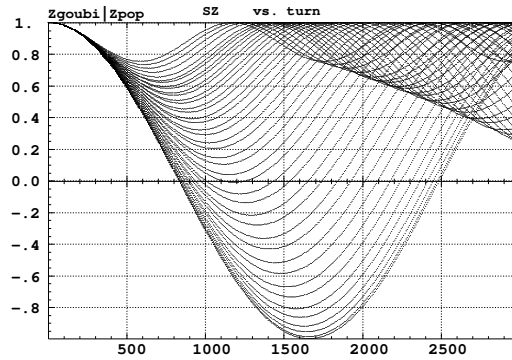
```

6123 - with BORO changed, closer to $G\gamma_R = 4 - \nu_y \approx 3.1115$, DIPOLE field needs to
6124 be set to 5.27284 kG,

6125 - a number of turns $IPASS \approx$ a few thousand, under REBELOTE, results in
6126 at least half an oscillation of $S_Z(turn)$ (the precession frequency increases with
6127 the distance to the resonance, with a minimum of $\omega = |\epsilon_R|$ on the resonance [8,
6128 Fig. 3.4]), which is convenient for determining $\langle S_Z \rangle$.

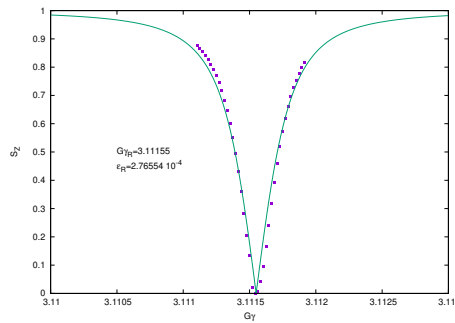
6129 Figure 17.68 displays the turn-by-turn evolution of the vertical component of
6130 the spins as they precess around the eigenvector \mathbf{n} (Eq. 9.20). A quick, and ac-

Fig. 17.68 Turn-by-turn value of the vertical component of spins precessing at fixed energy in SATURNE I synchrotron, observed at the beginning of the sequence, where spins start vertical ($S_Z = 1$). The greater (respectively smaller) the distance to the resonance, the closer the precession axis is to the vertical (resp., to the bend plane), and the greater (resp. the smaller) the oscillation frequency $\omega = \sqrt{\Delta^2 + |\epsilon_R|^2}$



6131 curate enough, approximation to the vertical component of the precession axis
 6132 is $\langle S_Z \rangle_{\text{period}} = \frac{1}{2} \{ \min [S_Z(\theta)] + \max [S_Z(\theta)] \}$, it yields the $\langle S_Z \rangle (\Delta)$ graph of Fig. 17.69.

Fig. 17.69 Vertical component of the spin precession axis as a function of $G\gamma$, in the vicinity of the resonance. Markers are from tracking, solid curve and numerical values of $G\gamma_R$ and ν_Z are from a match using Eq. 9.37



6133 A match of the $\langle S_Z \rangle$ values by (Eq. 9.37)

$$S_y(\Delta) = \frac{\Delta}{\sqrt{\Delta^2 + |\epsilon_R|^2}}$$

given $G\gamma_R = 4 - \nu_Z$, yield vertical tune and resonance strength values, respectively,

$$\nu_Z = 0.88845 \quad \text{and} \quad |\epsilon_R| = 2.77 \times 10^{-4}$$

6134 Satisfactorily, ν_Z is consistent with earlier results, and $|\epsilon_R| = 2.77 \times 10^{-4}$ for
 6135 $\epsilon_Z/\pi = 79 \times 10^{-6}$ here, is consistent in order of magnitude with $|\epsilon_R| = 2.44 \times 10^{-5}$
 6136 for $\epsilon_Z/\pi = 10^{-6}$ in the previous question (h). The difference deserves further
 6137 inspection, a possible additional question in this exercise.

6138 (i) Bunch depolarization.

Spin depolarizing resonances in SATURNE I synchrotron are located at (Figs. 17.70, 17.71)

$$G\gamma_R = k \pm \nu_Z = k \pm 0.888284 \quad \equiv 4 - 0.888284, 4 + 0.888284, 8 - 0.888284$$

6139 where ν_Z has been taken from Tab. 17.51, or from Fig. 17.64. $G\gamma_R$ is bounded by
6140 $G\gamma(3 \text{ GeV}) = 7.525238 < 8 + \nu_Z$

6141 The simulation data file to track through these resonances is the same as in
6142 question (e), Tab. 17.55, except for the following:

- 6143 - substitute MCOBJET (to be uncommented) to OBJET (to be commented),
- 6144 - under CAVITE substitute a peak voltage $V = 20 \text{ kV}$ to $V = 200 \text{ kV}$,
- under REBELOTE, request a 300,000 turn cycle rather than 30,000.

MCOBJET creates a 200 particle bunch with Gaussian transverse and longitudinal densities, with the following *rms* values at 3.6 MeV:

$$\varepsilon_Y/\pi = 25 \mu\text{m}, \quad \varepsilon_Z/\pi = 10 \mu\text{m}, \quad \frac{dp}{p} = 10^{-4}$$

6145 CAVITE accelerates that bunch from 3.6 MeV to 3 GeV at a rate of $q\hat{V} \sin(\phi_s) =$
6146 10 keV/turn ($\hat{V} = 20 \text{ kV}$, $\phi_s = 30^\circ$), in 300,000 turns.

6147 Figure 17.70 shows sample S_Z spin components of a few particles taken among
6148 the 200 tracked. Figure 17.71 displays $\langle S_Z \rangle$, the vertical polarization component of
6149 the 200 particle set. A gnuplot script is used, given in Tab. 17.59.

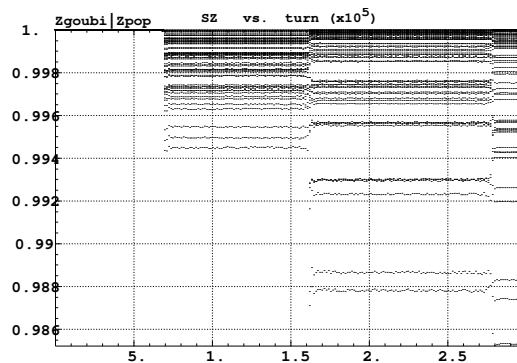


Fig. 17.70 Vertical spin component of a few particles accelerated from 3.6 MeV to 3 GeV. A graph obtained using zpop, data read from [b_]zgoubi.fai: menu 7; 1/2 to open b_zgoubi.fai; 2/[20,23] for S_Z versus turn; 7 to plot

6150 The strength of any one of the three resonances crossed can be computed, from
6151 the upstream and downstream bunch polarization averaged over the 200 particles,
6152 using Eq. 17.15. Dependence upon the vertical emittance of the bunch can be
6153 performed repeating this tracking simulation, with a different vertical emittance
6154 (under MCOBJET).

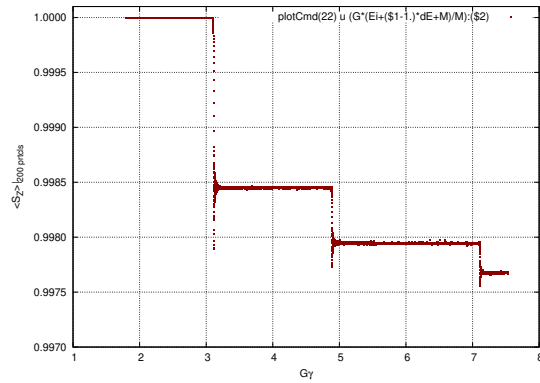


Fig. 17.71 Average vertical spin component of a 200 particle bunch, accelerated from 3.6 MeV to 3 GeV

Table 17.59 A gnuplot script to plot the average vertical spin component of the 200 particle set, along the acceleration ramp (Fig. 17.71). The average is prior computed by an awk script, which reads the necessary data from zgoubi.fai.

```
# gnuplot_avrgFromFai.gnu
 fName = 'zgoubi.fai'; plotCmd(col_num)=sprintf('< gawk -f average.awk -v col_num=%d %s', col_num, fName)
 set xtics; set ytics; set xlabel "G{/Symbol g}"; set ylabel "<S_z>|_{200 prtcls}"
 set format y "%.4f"; set grid; set xr [:]; set yr [1.997:1.0001]
 Qy=0.888248;
 do for [intgr=1:2] { set arrow nohead from 4*intgr-Qy, 0.997 to 4*intgr+Qy, 1.0001 lw 1 dt 2
                    set arrow nohead from 4*intgr+Qy, 0.997 to 4*intgr+Qy, 1.0001 lw 1 dt 2 }
 M=938.27208; Ei = 3.6; G = 1.79284735; Qy = 0.888248; dE = 0.01 # MeV/turn
 plot plotCmd(22) u (G*(Ei+($1-1)*dE+M)/M):($2) w p pt 5 ps .4 lc rgb 'dark-red'; pause 1
```

average.awk script to compute $\langle S_z \rangle$ [5]:

```
function average(x, data){
  n = 0; mean = 0;
  val_min = 0; val_max = 0;
  for(val in data){
    n += 1;
    delta = val - mean;
    mean += delta/n;
    val_min = (n == 1)?val:((val < val_min)?val:val_min);
    val_max = (n == 1)?val:((val > val_max)?val:val_max);
  }
  if(n > 0){
    print x, mean, val_min, val_max;
  }
}
{
  curr = $38;
  yval = $(col_num);

  if(NR==1 || prev != curr){
    average(prev, data);
    delete data;
    prev = curr; }
  data[yval] = 1; }
END{
  average(curr, data); }
```

6155 Checking dependence upon crossing speed of the depolarizing effect of the res-
6156 onances can be performed by repeating this tracking simulation with a different
6157 accelerating rate $\hat{V} \sin(\phi_s)$.

6158 **9.2 Construct the ZGS. Spin Resonances**

6159 (a) A model of ZGS synchrotron.

6160 DIPOLE is used to simulate both cell dipoles. It is necessary to have Fig. 17.55
6161 at hand (in addition to the users' guide), when filling up the data list under DIPOLE.
6162 Some comments regarding these data:

- 6163 • DIPOLE field is defined in a cylindrical coordinate system.
- 6164 • The bending sector is 45 degrees, this is also the field region extent angle AT in
6165 the preliminary hard-edge model.
- 6166 • When accounting for fringe fields, the angular extent AT has to encompass the
6167 fringe fields, at both ends of the 45 deg sector: an extra 5 deg takes care of that,
6168 for a total $AT=55$ deg, which ensures absence of truncation of the fringe fields at
6169 the AT sector boundaries, over the all radial excursion of the beam.
- 6170 • RM is given the curvature radius value, $RM = B\rho/B = 1.035270_{[Tm]}/0.04986851_{[T]} =$
6171 20.76 m, this makes magnet positioning and closed orbit checks easier (see be-
6172 low).
- 6173 • The field and reference rigidity are for injection energy, 50 MeV, an arbitrary
6174 choice.
- 6175 • $ACENT=27.5$ deg is the reference azimuth for the positioning of the entrance and
6176 exit EFBs. It is taken in the middle of the AT range, an arbitrary choice.
- 6177 • The entrance radius in the AT sector is $RE = RM/\cos(AT - \omega^+) = RM/\cos(5^\circ)$,
6178 with $\omega^+ = 22.5$ deg the positioning of the entrance EFB with respect to $ACENT$
6179 (Fig. 17.55). And similarly for the positioning of the exit reference frame,
6180 $RS = RM/\cos(AT - (ACENT - \omega^-)) = RM/\cos(5^\circ)$ with $\omega^- = -22.5$ deg
6181 the positioning of the exit EFB. Note that $\omega^+ - \omega^- = 45^\circ$, the value of the bend
6182 angle.
- 6183 • The entrance angle TE identifies with the extension to the 45 deg sector, namely,
6184 $TE=5$ deg. And similarly for the positioning of exit frame, 5 deg downstream of
6185 the exit EFB, $TS=5$ deg.

6186 In order to build the cell, and in the first place the two cell dipoles (they are mirror
6187 symmetric, thus build one, the other follows), it is a good idea to proceed by steps:

6188 (i) first build a 45 deg sector in the hard edge model (Tab. 17.60). Outcomes of
6189 FAISCEAU located next to DIPOLE indicate that a trajectory entering DIPOLE at
6190 radius $R = RM$, normal to the EFB (thus, $Y_0 = 0$ and $T_0 = 0$ in OBJET), exits
6191 with $Y=0$ and $T=0$. Data validation at this stage can be performed by comparing
6192 DIPOLE's transport matrix computed with MATRIX, and the theoretical expectation
6193 (after Eq. 15.6):

$$T = \begin{pmatrix} \cos \alpha & \rho \sin \alpha & 0 & 0 & 0 & \rho(1 - \cos \alpha) \\ -\frac{1}{\rho} \sin \alpha & \cos \alpha & 0 & 0 & 0 & \sin \alpha \\ 0 & 0 & 1 & \rho \alpha & 0 & 0 \\ 0 & 0 & 0 & 1 & 0 & 0 \\ \sin \alpha & 0 & 0 & 0 & 1 & \rho(\alpha - \sin \alpha) \\ 0 & 0 & 0 & 0 & 0 & 1 \end{pmatrix} \stackrel{\substack{\alpha=\pi/4, \\ \rho=20.76}}{=} \begin{pmatrix} 0.7071 & 14.6795 & 0 & 0 & 0 & 6.0804 \\ -0.03406 & 0.7071 & 0 & 0 & 0 & 0.7071 \\ 0 & 0 & 1 & 16.3048 & 0 & 0 \\ 0 & 0 & 0 & 1 & 0 & 0 \\ 0.7071 & 0 & 0 & 0 & 1 & 1.6253 \\ 0 & 0 & 0 & 0 & 0 & 1 \end{pmatrix}$$

6194 MATRIX computation outcomes from raytracing can be found for comparison in
6195 Tab. 17.61.

Table 17.60 Simulation input data file: a 45 degree sector bend in the hard edge model. The reference trajectory has equal entrance and exit position, and opposite sign angles. It coincides with the arc $R = RM$. MATRIX computes the transport matrix of the dipole (bottom of this Table), for comparison with the fringe field model

```
ZGS. Hard edge dipole model. Transport matrix.
'OBJET'
1.03527036749193e3
5
! Create a 13 particle set, proper for MATRIX computation.
! Reference Brho: 50 MeV proton.
! Coordinate sampling.
.001 .01 .001 .01 .001 .0001
0. 0. 0. 0. 0. 1.
! Reference trajectory: all initial coordinates nul, relative rigidity D=1.
1
'DIPOLE'
! Analytical modeling of a dipole magnet.
20
! IL=2 here, to log trajectory coordinates in zgoubi.plt, at integration steps.
45. 2076.
! Field region angle=45; reference radius set to curvature radius value.
22.5 0.4986851481175 0. 0. 0.
! Reference angle ACENT set to AT/2; Bo field at RM; indices, all zero.
0. 0.
! EFB 1, hard-edged.
4 .1455 2.2670 -.6395 1.1558 0. 0.
! Edge coefficients.
22.5 0. 1.E6 -1.E6 1.E6 1.E6
! Angle to ACENT; face angle; face is straight.
0. 0.
! EFB 2, hard-edged.
4 .1455 2.2670 -.6395 1.1558 0. 0.
-22.5 0. 1.E6 -1.E6 1.E6 1.E6
! EFB 3. Unused.
0. 0.
0. 0. 0. 0. 0. 0.
0. 0. 1.E6 -1.E6 1.E6 1.E6
2 1
! Degree of interpolation polynomial; flying grid sizing.
200.
! Integration step size. It can be large in uniform field.
2 2076. 0. 2076. 0.
! Positioning of entrance and exit frames.
! reference frames.
'FAISCEAU'
! Local particle coordinates.
'MATRIX'
! Compute transport matrix, from trajectory coordinates.
1 0
'END'
```

6196 (ii) next, add fringe fields, including the 5 deg extensions that add to AT
6197 (Tab. 17.62). Negative drifts with length $RM \tan(5^\circ) = 181.62646548$ cm have
6198 been added at both ends, so to recover the actual 45 deg sector opening. A FIT
6199 procedure finds the field value necessary for recovering the exact orbit deviation,
6200 as the latter is perturbed when introducing fringe fields. Again, FAISCEAU allows
6201 checking the correctness of DIPOLE data: exit coordinates come out to be $Y=0$ and
6202 $T=0$; however the path across the dipole is changed under the effect of the fringe
6203 fields, thus its length: $s=1630.459$ cm is slightly different, compared to the hard edge
6204 case (an arc of radius radius $RM=2076$ cm and length 1630.487 cm)

(iii) next, add the EFB angles: the sector is closing (wedge angles $\varepsilon_1 > 0$ and $\varepsilon_2 > 0$ by convention) thus the EFB tilt angle θ under DIPOLE if positive at entrance, negative at exit (Fig. 17.55). In order to reach proper wave number values (this is addressed below), the wedge angles are taken to be $\varepsilon_1 = 13^\circ$ and $\varepsilon_2 = 8^\circ$. These considerations result in the following:

- the entrance (respectively exit) EFB of the upstream dipole of the cell (Fig. 9.24) is tilted with respect to the reference orbit by an angle $\theta = +13^\circ$ (resp. $\theta = -8^\circ$),
- the entrance (resp. exit) EFB of the downstream dipole is tilted with respect to the reference orbit by an angle $\theta = +8 \text{ deg}$ (resp. $\theta = -13^\circ$).

This final step requires again re-adjusting the radial positioning of the dipole (RE and RS, entrance and exit radius respectively), and field. In that aim the FIT procedure in Tab. 17.62 is added a variable: the RE and RS radii, coupled, and a constraint: the reference orbit has zero radial excursion at exit of the dipole. This FIT results in re-adjusted magnetic field and RE, RS positioning, with the respective values

Table 17.61 Outcomes of the simulation file of Tab. 17.60

An excerpt from *zgoubi.res* execution listing. Coordinates of the first particle (the reference trajectory) and its path length under FAISCEAU, at OBJET on the left hand side below, locally on the right hand side:

```

3 Keyword, label(s) : FAISCEAU
                                TRACE DU FAISCEAU
                                (follows element # 2)
                                13 TRAJECTOIRES
                                OBJET
                                FAISCEAU
0 1 D Y(cm) T(mr) Z(cm) P(mr) S(cm) D-1 Y(cm) T(mr) Z(cm) P(mr) S(cm)
    1.0000 0.000 0.000 0.000 0.000 0.0000 0.0000 -0.000 -0.000 0.000 0.000 1.630487E+03

```

Transport matrix of a 45 degree sector, hard edge model, two difference cases of integration step size, namely, 4 cm and 2 m (an excerpt of MATRIX computation, from *zgoubi.res* execution listing). It can be checked against matrix transport expectations. The “first order symplectic conditions” are very small in the 4 cm step size case, which is an indication of accurate numerical integration of the trajectories across DIPOLE; the reference trajectory (first one) exits better aligned (reference coordinates, before change of frame for MATRIX computation, are closer to zero):

- Case of 4 cm step size:

```

4 Keyword, label(s) : MATRIX
Reference, before change of frame (particle # 1 - D-1,Y,T,Z,s,time) :
0.00000000E+00 -3.25144356E-10 -4.13789229E-10 0.00000000E+00 0.00000000E+00 1.63048659E+03 5.43871783E-02

TRANSFER MATRIX ORDRE 1 (MKSA units)
0.707107 14.6795 0.00000 0.00000 0.00000 6.08046
-3.406102E-02 0.707107 0.00000 0.00000 0.00000 0.707107
0.00000 0.00000 1.00000 16.3049 0.00000 0.00000
0.00000 0.00000 7.285552E-16 1.00000 0.00000 0.00000
0.707107 6.08046 0.00000 0.00000 1.00000 1.62533
0.00000 0.00000 0.00000 0.00000 0.00000 1.00000

DetY-1 = 0.00000000025, DetZ-1 = 0.00000000002
T12=0 at -20.76 m, T34=0 at -16.30 m
First order symplectic conditions (expected values = 0) :
2.5100E-09 2.3381E-10 0.000 0.000 0.000 0.000

```

- Case of 2 m step size:

```

4 Keyword, label(s) : MATRIX
Reference, before change of frame (particle # 1 - D-1,Y,T,Z,s,time) :
0.00000000E+00 -2.01277929E-03 -2.51514609E-03 0.00000000E+00 0.00000000E+00 1.63048722E+03 5.43871994E-02

TRANSFER MATRIX ORDRE 1 (MKSA units)
0.707105 14.6795 0.00000 0.00000 0.00000 6.08056
-3.406102E-02 0.707108 0.00000 0.00000 0.00000 0.707120
0.00000 0.00000 1.00000 16.3051 0.00000 0.00000
0.00000 0.00000 1.457135E-17 1.00003 0.00000 0.00000
0.707109 6.08048 0.00000 0.00000 1.00000 1.62531
0.00000 0.00000 0.00000 0.00000 0.00000 1.00000

DetY-1 = -0.0000010903, DetZ-1 = 0.0000286273
R12=0 at -20.76 m, R34=0 at -16.30 m
First order symplectic conditions (expected values = 0) :
-1.0903E-06 2.8627E-05 0.000 0.000 0.000 0.000

```

$$B_0 = 0.49860858 \text{ kG} \quad \text{and} \quad RE = RS = 2084.5090 \text{ cm}$$

6205 This is the values used in the ZGS cell simulation in Tab. 17.63,

6206 (iv) and, finally, assemble this dipole and its mirror symmetric, in a cell (Fig. 9.24
6207 and Tab. 17.63). The mirror symmetric is obtained by just permuting the entrance
6208 and exit wedge angles. The cell includes a half long-drift at each end, and a short
6209 drift between the dipoles. The three have been taken equal for simplification, 3.37 m
6210 long.

Table 17.62 Simulation input data file: ZGS 45deg sector bend, with entrance and exit EFBs wedge angles and fringe fields. The reference trajectory has equal entrance and exit position, and opposite sign angles. It runs closely to the arc $R = RM$, not strictly coinciding with the latter due to the fringe fields. MATRIX computes the transport matrix of the dipole, for comparison with the hard edge model. Negative drifts with length $RM \tan(5^\circ) = 181.62646548$ cm are added to recover the hard edge path length

```
ZGS. Simplified model. Find centered orbit in DIPOLE.
'OBJET'
1.03527036749193e3                                     ! Reference Brho: 50 MeV proton.
5                                                         ! Create a 13 particle set, proper for MATRIX computation.
.001 .01 .001 .01 .001 .0001                             ! Coordinate sampling.
0. 0. 0. 0. 0. 1.                                       ! Reference trajectory: all initial coordinates nul, relative rigidity D=1.
1
'DRIFT'
-181.62646548
'DIPOLE'
0                                                         ! Analytical modeling of a dipole magnet.
! IL=2 here, to log trajectory coordinates in zgoubi.plt, at integration steps.
55. 2076.                                                ! Field region angle=45; reference radius set to curvature radius value.
27.5 0.49860858 0. 0. 0.                                ! Reference angle ACENT set to AT/2; Bo field at RM; indices, all zero.
60. 0.                                                    ! EFB 1 with fringe field extent.
4 .1455 2.2670 -.6395 1.1558 0. 0. 0.                 ! Enge coefficients.
22.5 13. 1.E6 -1.E6 1.E6 1.E6                          ! EFB angle to ACENT; 13 deg EFB tilt angle; EFB is straight.
60. 0.                                                    ! EFB 2 with fringe field extent.
4 .1455 2.2670 -.6395 1.1558 0. 0. 0.                 ! Enge coefficients.
-22.5 -8. 1.E6 -1.E6 1.E6 1.E6                         ! EFB angle to ACENT; -8 deg EFB tilt angle; EFB is straight.
0. 0.                                                    ! EFB 3. Unused.
0. 0. 0. 0. 0. 0. 0. 0. 0. 0. 0. 0. 0. 0.
0. 0. 1.E6 -1.E6 1.E6 1.E6 0.
2 1                                                       ! Degree of interpolation polynomial; flying grid sizing is step, proper for accuracy.
4.0                                                       ! Integration step size.
2 2084.5090 -0.087266462599717 2084.5090 0.087266462599717 ! Positioning of entrance and exit.
'DRIFT'
-181.62646548
'FIT'
2
3 5 0 .1                                                  ! Vary DIPOLE field.
3 64 3.66 .1
2 1e-15 999
3 1 2 #End 0. 1. 0                                       ! Request nul trajcory position at exit of DIPOLE.
3 1 3 #End 0. 1. 0                                       ! Request nul trajcory angle at exit of DIPOLE.

'FAISCEAU'                                               ! Local particle coordinates.
'MATRIX'                                                 ! Compute transport matrix, from trajectory coordinates.
1 0
'END'
```

An excerpt from zgoubi.res execution listing. Coordinates of the first particle (the reference trajectory) and its path length, under FAISCEAU, at OBJET on the left hand side, locally on the right hand side:

```
5 Keyword, label(s) : FAISCEAU
                                TRACE DU FAISCEAU
                                (follows element # 4)
                                13 TRAJECTOIRES
                                OBJET
                                D          Y(cm)    T(mr)    Z(cm)    P(mr)    S(cm)    D-1    Y(cm)    T(mr)    Z(cm)    P(mr)    S(cm)
0 1 1.0000 0.000 0.000 0.000 0.000 0.0000 0.0000 -0.000 -0.000 0.000 0.000 1.630459E+03 1
```

Transport matrix of ZGS 45 degree sector with EFB wedge angles and fringe fields (an excerpt of MATRIX computation, from zgoubi.res execution listing). It can be checked against matrix transport expectations. The “first order symplectic conditions” are small, which is an indication of accurate numerical integration of the trajectories across DIPOLE:

```
7 Keyword, label(s) : MATRIX
Reference, before change of frame (particle # 1 - D-1,Y,T,Z,s,time) :
0.00000000E+00 -2.19331903E-08 -2.24434360E-08 0.00000000E+00 0.00000000E+00 1.63080750E+03 6.65146963E-02

TRANSFER MATRIX ORDRE 1 (MKSA units)
0.870365 14.6806 0.00000 0.00000 0.00000 6.08068
-2.030224E-02 0.806593 0.00000 0.00000 0.00000 0.748209
0.00000 0.00000 0.827040 16.3143 0.00000 0.00000
0.00000 0.00000 0.00000 -1.580329E-02 0.897394 0.00000
0.774666 6.08004 0.00000 0.00000 1.00000 1.63006
0.00000 0.00000 0.00000 0.00000 0.00000 1.00000

DetY-1 = -0.0000003451, DetZ-1 = 0.0000000379
T12=0 at -18.20 m, T34=0 at -18.18 m
First order symplectic conditions (expected values = 0) :
-3.4507E-07 3.7861E-08 0.000 0.000 0.000 0.000
```

Table 17.63 Simulation input data file: ZGS cell simplified model, obtained by assembling DIPOLE taken from Tab. 17.62 and its mirror symmetric (which means, permuting entrance and exit EFB tilt angles θ), and adding drift spaces. This input data file defines the ZGS cell sequence segment S_ZGS_cell to E_ZGS_cell, for possible use in INCLUDE statements in subsequent exercises. It also defines, for the same purpose, the dipoles sequence segments S_ZGS-DIP_UP to E_ZGS-DIP_UP (first dipole of the cell) and S_ZGS-DIP_DW to E_ZGS-DIP_DW (second dipole of the cell). In these possible INCLUDE statements, this file is used under the name ZGS_cell.inc

```

File ZGS_cell.INC.dat.
! ZGS. Simplified model, 8-periodic.
'MARKER' ZGSCellMATRIX_S                               ! Just for edition purposes.
'OBJET'
1.03527036749193e3                                     ! Reference Brho: 50 MeV proton.
5                                                         ! Create a 13 particle set, proper for MATRIX computation.
.001 .01 .001 .01 .001 .0001                             ! Coordinate sampling.
0. 0. 0. 0. 0. 1.   ! Reference trajectory: all initial coordinates nul, relative rigidity D=1.
1
'MARKER' S_ZGS_cell                                     ! ZGS cell begins here.
'DRIFT' half_longDrift
337.
'MARKER' S_ZGS-DIP_UP                                   ! 1st dipole of cell begins here.
'DRIFT'
-181.62646548
'DIPOLE' DIP_UP                                         ! Analytical modeling of a dipole magnet.
2                                                         ! IL=2 here, to log trajectory coordinates in zgoubi.plt, at integration steps.
55. 2076.                                                ! Field region angle=45; reference radius set to curvature radius value.
27.5 0.49860858 0. 0. 0.   ! Reference angle ACENT set to AT/2; Bo field at RM; indices, all zero.
60. 0.                                                    ! EFB 1 with fringe field extent.
4 .1455 2.2670 -.6395 1.1558 0. 0. 0.   ! Enge coefficients.
22.5 13. 1.E6 -1.E6 1.E6 1.E6   ! EFB angle to ACENT; EFB tilt angle; EFB is straight.
60. 0.                                                    ! EFB 2 with fringe field extent.
4 .1455 2.2670 -.6395 1.1558 0. 0. 0.   ! Enge coefficients.
-22.5 -8. 1.E6 -1.E6 1.E6 1.E6   ! EFB angle to ACENT; EFB tilt angle; EFB is straight.
0. 0. 0. 0. 0. 0. 0. 0. 0. 0. 0. 0. 0.   ! EFB 3. Unused.
0. 0. 1.E6 -1.E6 1.E6 1.E6 0.
2 1   ! Degree of interpolation polynomial; flying grid sizing is step, proper for accuracy.
2.0   ! Integration step size.
2 2084.5090 -0.087266462599717 2084.5090 0.087266462599717   ! Positioning of entrance and exit.
'DRIFT'
-181.62646548
'MARKER' E_ZGS-DIP_UP                                   ! 1st dipole of cell ends here.
'DRIFT' shortDrift
337.
'MARKER' S_ZGS-DIP_DW                                   ! 2nd dipole of cell begins here.
'DRIFT'
-181.62646548
'DIPOLE' DIP_DW                                         ! Analytical modeling of a dipole magnet.
2                                                         ! IL=2 here, to log trajectory coordinates in zgoubi.plt, at integration steps.
55. 2076.                                                ! Field region angle=45; reference radius set to curvature radius value.
27.5 0.49860858 0. 0. 0.   ! Reference angle ACENT set to AT/2; Bo field at RM; indices, all zero.
60. 0.                                                    ! EFB 1 with fringe field extent.
4 .1455 2.2670 -.6395 1.1558 0. 0. 0.   ! Enge coefficients.
22.5 8. 1.E6 -1.E6 1.E6 1.E6   ! EFB angle to ACENT; EFB tilt angle; EFB is straight.
60. 0.                                                    ! EFB 2 with fringe field extent.
4 .1455 2.2670 -.6395 1.1558 0. 0. 0.   ! Enge coefficients.
-22.5 -13. 1.E6 -1.E6 1.E6 1.E6   ! EFB angle to ACENT; EFB tilt angle; EFB is straight.
0. 0. 0. 0. 0. 0. 0. 0. 0. 0. 0. 0. 0.   ! EFB 3. Unused.
0. 0. 1.E6 -1.E6 1.E6 1.E6 0.
2 1   ! Degree of interpolation polynomial; flying grid sizing is step, proper for accuracy.
2.0   ! Integration step size.
2 2084.5090 -0.087266462599717 2084.5090 0.087266462599717   ! Positioning of entrance and exit.
'DRIFT'
-181.62646548
'MARKER' E_ZGS-DIP_DW                                   ! 2nd dipole of cell ends here.
'DRIFT' half_longDrift
337.
'MARKER' E_ZGS_cell                                     ! ZGS cell ends here.
'FAISCEAU'                                             ! Local particle coordinates.
'TWISS' ! Produce transport matrix, beam matrix, and periodic optical functions along the sequence.
2 1. 1.
'MARKER' ZGSCellMATRIX_E                               ! Just for edition purposes.
'END'
ZGS. Simplified model, 8-periodic.

```

An excerpt from zgoubi.res execution listing. Coordinates of the first particle (the reference trajectory) and its path length, under FAISCEAU, at OBJET on the left hand side, locally on the right hand side:

```

18 Keyword, label(s) : FAISCEAU
                                TRACE DU FAISCEAU
                                (follows element # 4)
                                13 TRAJECTOIRES
                                OBJET
                                FAISCEAU
                                D      Y(cm)  T(mr)  Z(cm)  P(mr)  S(cm)  D-1  Y(cm)  T(mr)  Z(cm)  P(mr)  S(cm)
0 1 1.0000 0.000 0.000 0.000 0.000 0.0000 0.0000 -0.000 -0.000 0.000 0.000 4.272614E+03

```

6211 *Lattice parameters*

6212 The TWISS command down the sequence (Tab. 17.63) produces the periodic beam matrix results shown in Tab. 17.64

Table 17.64 Results obtained running the simulation input data file of Tab. 17.63, ZGS cell - an excerpt from zgoubi.res execution listing

```

13 Keyword, label(s) : TWISS
Reference, before change of frame (particle # 1 - D-1,Y,T,Z,s,time) :
0.00000000E+00 -1.59240732E-05 -9.81570020E-07 0.00000000E+00 0.00000000E+00 4.27261430E+03 4.53811009E-01

Beam matrix (beta/-alpha/-alpha/gamma) and periodic dispersion (MKSA units)
28.633680 0.000002 0.000000 0.000000 0.000000 36.853463
0.000002 0.034924 0.000000 0.000000 0.000000 0.000003
0.000000 0.000000 37.008846 0.000001 0.000000 -0.000000
0.000000 0.000000 0.000001 0.027021 0.000000 0.000000
0.000000 0.000000 0.000000 0.000000 0.000000 0.000000
0.000000 0.000000 0.000000 0.000000 0.000000 0.000000

Betatron tunes (Q1 Q2 modes)
NU_Y = 0.21235913 NU_Z = 0.19286706

Momentum compaction :
dL/L / dp/p = 1.4126935
(dp = 0.000000E+00 L(0) = 4.27261E+03 cm, L(0)-L(-dp) = 6.03584E-01 cm, L(0)-L(+dp) = -6.03595E-01 cm)

Transition gamma = 8.41348710E-01

Chromaticities :
dNu_y / dp/p = 4.70986585E-02 dNu_z / dp/p = 4.45745634E-02

```

6213

6214 The TWISS command also produces a zgoubi.TWISS.out file which details the
6215 optical functions along the sequence (at the downstream end of the optical elements).

6216 The header of that file details the optical parameters of the structure (Tab. 17.65).

Table 17.65 An excerpt of zgoubi.TWISS.out file resulting from the execution of the ZGS cell simulation input data file of Tab. 17.63. Note that the ring (4-period) wave numbers are 4 times the cell values Q1, Q2 displayed here. Optical functions (betatron function and derivative, orbit, phase advance, etc.) along the optical sequence are listed as part of zgoubi.TWISS.out following the header. The top part and last line of that listing are given below

```

@ LENGTH           %le  42.72614305
@ ALFA             %le  1.412693458
@ ORBIT5          %le  -0
@ GAMMATR         %le  0.8413487096
@ Q1               %le  0.2123591260 [fractional]
@ Q2               %le  0.1928670550 [fractional]
@ DQ1             %le  0.4709865847E-01
@ DQ2             %le  0.4457456345E-01
@ DXMAX           %le  3.81566835E+01 @ DXMIN           %le  3.68534544E+01
@ DYMAY           %le  0.00000000E+00 @ DYMIN           %le  0.00000000E+00
@ XCOMAX          %le  3.68530296E-01 @ XCOMIN          %le  -1.59240732E-07
@ YCOMAX          %le  0.00000000E+00 @ YCOMIN          %le  0.00000000E+00
@ BETXMAX         %le  3.25272034E+01 @ BETXMIN         %le  2.86307346E+01
@ BETYMAX         %le  3.73198843E+01 @ BETYMIN         %le  3.50936471E+01
@ XCORMS          %le  8.67153286E-04
@ YCORMS          %le  0.
@ DXRMS           %le  6.22665688E-01
@ DYRMS           %le  0.00000000E+00

```

Top and bottom four lines (truncated) of zgoubi.TWISS.out optical functions listing, including the periodic β_x , β_y (β_Y , β_Z in zgoubi notations) and D_x (η_Y in zgoubi notations) values at cell ends:

```

# alfx      btx      alfy      bty      alfl      btl      Dx      Dxp
-2.2668087e-6  2.8636996e+1 -1.0203802e-6  3.7013045e+1  0.0000000e+0  0.0000000e+0  3.6856253e+1  1.2733594e-4 etc.
-2.2589191e-6  2.8636995e+1 -9.9937511e-7  3.7013042e+1  0.0000000e+0  0.0000000e+0  3.6853463e+1  2.6012859e-6 etc.
-2.2589191e-6  2.8636995e+1 -9.9937511e-7  3.7013042e+1  0.0000000e+0  0.0000000e+0  3.6853463e+1  2.6012859e-6 etc.
-1.1768220e-1  2.9033592e+1 -9.1049986e-2  3.7319884e+1  0.0000000e+0  0.0000000e+0  3.6853472e+1  2.6012859e-6 etc.
.....
1.1775697e-1  2.9027748e+1  9.1140989e-2  3.7313084e+1  0.0000000e+0  0.0000000e+0  3.6853454e+1  2.6012859e-6 etc.
1.1775697e-1  2.9027748e+1  9.1140989e-2  3.7313084e+1  0.0000000e+0  0.0000000e+0  3.6853454e+1  2.6012859e-6 etc.
5.1297527e-5  2.8630735e+1  7.3912348e-5  3.7005690e+1  0.0000000e+0  0.0000000e+0  3.6853463e+1  2.6012859e-6 etc.
5.1297527e-5  2.8630735e+1  7.3912348e-5  3.7005690e+1  0.0000000e+0  0.0000000e+0  3.6853463e+1  2.6012859e-6 etc.

```

6217 (b) Betatron functions of the ZGS cell.

6218 Among the various ways to produce the betatron functions along the sequence
6219 (and throughout the DIPOLES), here are two possibilities, based on the storage of
6220 particle coordinates in zgoubi.plt during stepwise raytracing:

- 6221 1. a direct way consists in using OBJET[KOBJ=5] and transport the 13-particle
6222 set so obtained across the sequence; then, betaFromPlt from zgoubi toolbox [2]
6223 can be used to compute the transport matrix from the origin, step by step along
6224 the sequence, from particle coordinate values logged in zgoubi.plt during the
6225 stepwise integration;
- 6226 2. an indirect way consists in launching a few particles on a common invariant (hori-
6227 zontal and/or vertical) and subsequently plot the s -dependent quantities $\hat{Y}^2(s)/\varepsilon_Y$
6228 and/or $\hat{Z}^2(s)/\varepsilon_Z$. The maximum value of the latter, a function of the distance s ,
6229 is the betatron function along the sequence, $\beta_{Y,Z}(s)$.

6230 The second method is used here (this is an arbitrary choice. Exercises may be
6231 found in the various Chapters, that use the first method and may be referred to).

The input data file to derive the betatron function following method (2) above is given in Tab. 17.66. The initial ellipse parameters (under OBJET) are the periodic values, namely, $\alpha_Y = \alpha_Z = 0$, $\beta_Y = 28.63$ m, $\beta_Z = 37.01$ m, they are a sub-product of the TWISS procedure performed in (a), to be found in zgoubi.TWISS.out

(Tab. 17.65). The resulting envelopes and their squared value are shown in Fig. 17.72. Note that this raytracing also provides the coordinates of the 60 particles on their common upright invariant

$$x^2/\beta_x + \beta_x x'^2 = \varepsilon_x/\pi$$

6232 at start and at the end of the cell (with x standing for either Y or Z , and $\varepsilon_{Y,Z}/\pi =$
 6233 10^{-4} , here). This allows checking that the initial ellipse parameters (under OBJET,
 6234 Tab. 17.66) are effectively periodic values, and that the raytracing went correctly,
 6235 namely by observing that the initial and final ellipses do superimpose (Fig. 17.73).

Table 17.66 Simulation input data file: raytrace 60 particles across ZGS cell to generate beam envelopes. Store particle data in zgoubi.plt, along DRIFTS and DIPOLES. The INCLUDE file and segments are defined in Tab. 17.63

```
ZGS envelopes.
'OBJET'
1.03527036749193e3                               ! Reference Brho: 50 MeV proton.
8                                     ! Create a set of 60 particles evenly distributed on the same invariant;
1 60 1   ! case of 60 particles on a vertical invariant; use 60 1 1 instead for horizontal invariant.
0. 0. 0. 0. 0. 1.
0. 2.8637014E+1 0e-4
0. 3.7012633E+1 1e-4
0. 1. 0.

'FAISTORE'                                     ! This logs the coordinates of the particle to zgoubi.fai,
zgoubi.fai S_ZGS_cell E_ZGS_cell               ! at the two LABELs as indicated.
1

'MARKER' S_ZGS_cell
'DRIFT' half_longDrift                          ! Option 'split' divides the drift in 10 pieces,
337. split 10 2                                ! 'IL=2' causes log of particle data to zgoubi.plt.

'INCLUDE'
1
./ZGS_cell.inc[S_ZGS-DIP_UP:E_ZGS-DIP_UP]

'DRIFT' shortDrift
337. split 10 2

'INCLUDE'
1
./ZGS_cell.inc[S_ZGS-DIP_DW:E_ZGS-DIP_DW]

'DRIFT' half_longDrift
337. split 10 2
'MARKER' E_ZGS_cell

'FAISCEAU'
'END'
```

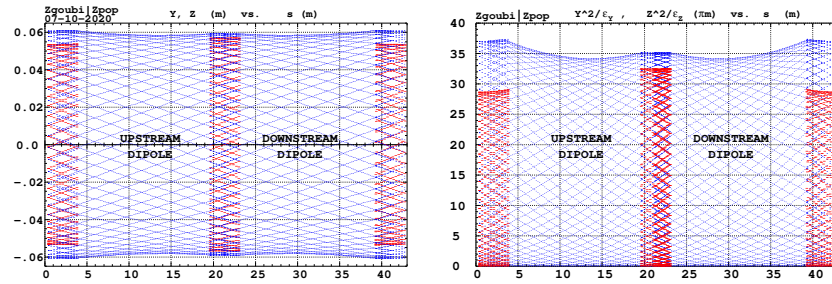



Fig. 17.72 Left: horizontal and vertical envelopes as generated by plotting the coordinates $Y(s)$ (thick lines, red, along the drifts only) or $Z(s)$ (thin lines, blue) across the ZGS cell, of 60 particles evenly distributed on a common $10^{-4} \pi m$ invariant, either horizontal or vertical (while the other invariant is zero). Right: a plot of $Y^2(s)/\epsilon_Y$ and $Z^2(s)/\epsilon_Z$: the extrema identify with $\hat{\beta}_Y(s)$ and $\hat{\beta}_Z(s)$, respectively. The extrema extremorum values are $\hat{\beta}_Y = 32.5$ m and $\hat{\beta}_Z = 37.1$ m, respectively. Graphs obtained using zpop, data read from zgoubi.plt: menu 7; 1/5 to open zgoubi.fai; 2/[6,2] (or [6,4]) for Y versus s (or Z versus s); 7 to plot; option 3/14 to raise Y (or Z) to the square

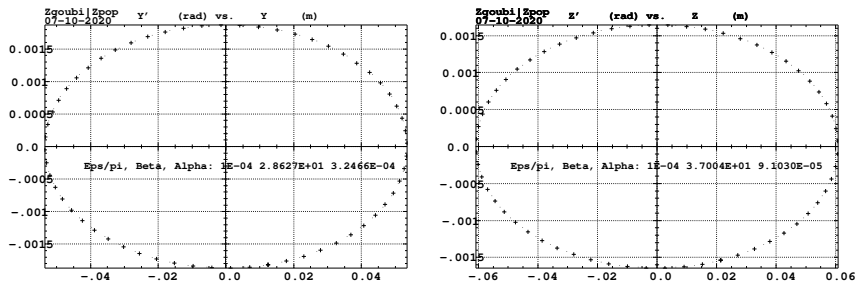


Fig. 17.73 Sixty particles evenly distributed on a common periodic invariant (of value either $\epsilon_Y = 10^{-4} \pi m$ and $\epsilon_Z = 0$, left graph, or the reverse, right graph) have been tracked from start to end of the cell. These periodic invariants are defined assuming the periodic ellipse parameters determined from prior TWISS, given in Tab. 17.65; values resulting from an *rms* match of the coordinates are given in the figure, and do agree with those TWISS data. The figure shows the good superposition of the start and end invariants (the start and end *rms* match ellipse parameters show negligible difference), which confirms the correct value of the periodic ellipse parameters, namely, left graph: horizontal phase space at start (crosses) and end (dots) of the cell; right graph: vertical phase space at start (crosses) and end (dots) of the cell

6236 *Dispersion function*

6237 Raytracing off-momentum particles on their chromatic closed orbit provides the
 6238 periodic dispersion function. In order to do so, the input data file of Tab. 17.66 can
 6239 be used, it just requires changing OBJET to the following:

```

6240 'OBJET'
6241 1.03527036749193e3 ! Reference Brho: 50 MeV proton.
6242 2 ! Create particles individually'
6243 3 1 ! three particles.
6244 +36.85e-1 0. 0. 0. 1.001 'p' ! Chromatic orbit coordinates Y0 and T0 for D=1.001 relative rigidity.
6245 0. 0. 0. 0. 1. 'o' ! On-momentum orbit.
6246 -36.85e-1 0. 0. 0. 0.999 'm' ! Chromatic orbit coordinates Y0 and T0 for D=0.999 relative rigidity.
6247 1 1 1
    
```

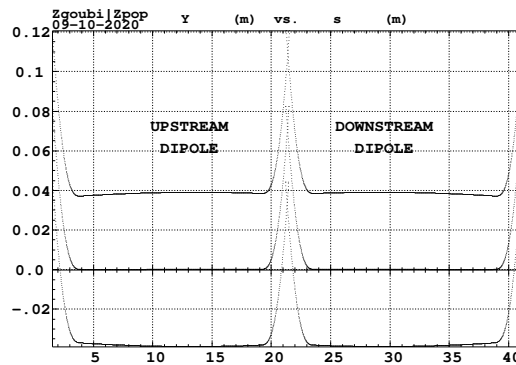
6248 The position and angle of the chromatic particles, which are offset by $\Delta p/p =$
 6249 $\pm 10^{-3}$, are drawn from the value of the periodic dispersion $\eta_Y = 36.85$ m and its
 6250 derivative $\eta'_Y \approx 0$ (Tab. 17.65), namely, $Y_0 = \eta_Y \Delta p/p = \pm 3.685$ cm and $T_0 =$
 6251 $\eta'_Y \Delta p/p = 0$.

6252 Running Tab. 17.66 simulation file with this new OBJET produces the following
 6253 coordinates at FAISCEAU, located at the end of the sequence (an excerpt from
 6254 zgoubi.res execution listing):

```
6255 18 Keyword, label(s) : FAISCEAU
6256
6257 TRACE DU FAISCEAU
6258 (follows element # 17)
6259 3 TRAJECTOIRES
6259
6260 OBJET FAISCEAU
6260
6261 D Y(cm) T(mr) Z(cm) P(mr) S(cm) D-1 Y(cm) T(mr) Z(cm) P(mr) S(cm)
6262 p 1 1.0010 3.685 0.000 0.000 0.000 0.0000 0.0010 3.685 0.000 0.000 0.000 4.278659E+03
6263 o 1 1.0000 0.000 0.000 0.000 0.000 0.0000 0.0000 0.000 0.000 0.000 0.000 4.272614E+03
6264 m 1 0.9990 -3.685 0.000 0.000 0.000 0.0000 -0.0010 -3.685 -0.000 0.000 0.000 4.266579E+03
```

6264 The local coordinates Y, T (under FAISCEAU, right hand side) are equal to the
 6265 initial coordinates Y_0, T_0 (under OBJET, left hand side), to better than $5 \mu\text{m}, 0.5 \mu\text{rad}$
 6266 accuracy respectively (zgoubi.fai can be consulted for greater precision on these
 6267 values), so confirming the periodicity of these chromatic trajectories. Figure 17.74
 6268 shows the particle trajectories through the two DIPOLES. A difference between the
 6269 on- and off-momentum trajectories yields as expected a quasi-constant $\eta_Y \approx 36.8$ m
 6270 whereas $\eta'_Y \approx 0$. η_Y departs from exactly zero due to the fringe fields and to the
 6271 wedge focusing.

Fig. 17.74 A graph of the radial excursion, within DIPOLE range (namely, $AT = 55^\circ$ extent, Tab. 17.63), of an on-momentum particle (its radial position in the dipole body is $R_0 \approx 20.7628$ m, corresponding to $Y=0$ in this graph) and two particles at respectively $dp/p = \pm 10^{-3}$. The diverging parts at DIPOLE ends are in the 5 deg fringe field regions. A graph obtained using zpop, data read from zgoubi.plt: menu 7; 1/1 to open zgoubi.plt; 2/[6,2] for Y versus distance; 7 to plot

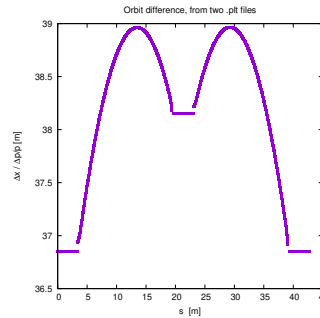


6272 *Orbit difference*

6273 The method can be used to compute the dispersion function, just like in machine
 6274 operation. This requires tracking a particle with $+dp/p$ momentum offset, save its
 6275 zgoubi.plt data (say, in zgoubi.plt+dpp), and repeat with $-dp/p$ (zgoubi.plt-dpp). A

6276 gnuplot script can compute and plot the orbit difference, and normalize to dp/p ; the result is the periodic dispersion, displayed in Fig. 17.75.

Fig. 17.75 Dispersion function along ZGS cell, obtained by orbit difference. The discontinuities are artifacts, they are located in the overlapping regions between the optical sequence DIPOLES and DRIFTS (Tab. 17.66)



6277

6278 (c) Some verifications regarding the model.

6279 The field along large excursion orbits can be logged in zgoubi.plt, using option
6280 IL=2 (or 20, or 200, etc. for printout every 10, or 100, etc. integration step) under
6281 DIPOLE.

6282 The simulation file of Tab. 17.66 is used to raytrace five particles, with OBJET
6283 changed to the following:

```
6284 'OBJET'
6285 1.03527036749193e3 ! Reference Brho: 50 MeV proton.
6286 2 ! Create particles individually,
6287 5 1 ! five particles.
6288 +36.85e-1 0. 0. 0. 1.01 'p' ! Chromatic orbit coordinates for D=1.01 relative rigidity.
6289 0. 0. 0. 0. 1. '0' ! On-momentum closed orbit.
6290 -36.85e-1 0. 0. 0. 0.99 'm' ! Chromatic orbit coordinates for D=0.99 relative rigidity.
6291 0. 0. 5. 0. 1. 'm' ! Initial vertical excursion is Z0= 5 cm off-mid-plane.
6292 0. 0. 20. 0. 1. 'm' ! Initial vertical excursion is Z0=20 cm off-mid-plane.
6293 1 1 1 1
```

6294 Apart from the on-momentum particle (2nd in the list) this OBJET defines two
6295 particles on $\Delta p/p = \pm 1\%$ chromatic orbit (1st and 3rd in the list), this is an excursion
6296 of a few tens of centimeters, large as requested, as $\Delta x \approx 38 \times dp/p$. OBJET also
6297 defines 2 particles launched into the cell at respectively $Z_0 = 5$ cm and $Z_0 = 20$ cm.

6298 The magnetic field as a function of the azimuthal angle in DIPOLE frame, along
6299 these trajectories across the upstream DIPOLE of the cell, is shown in Fig. 17.76.
6300 The field curves for the first four trajectories essentially superimpose except for the
6301 fringe field regions (Fig. 17.76), due to the wedge angles. This behaves as expected.
6302 Detail inspection is possible, from the detailed particle coordinate and field data in
6303 zgoubi.plt - this is out of the scope of the present question.

6304 The field along the 5th particle trajectory features overshoots (Fig. 17.76), this
6305 is due to the very large vertical excursion ($Z \approx 20$ cm in the entrance fringe field
6306 region). It looks reasonable, however it may be an artifact in the case that the high
6307 order derivatives of the field in that region are large, resulting from the truncated
6308 Taylor series method used for off mid-plane field extrapolation [1, Sect. 1.3.3].

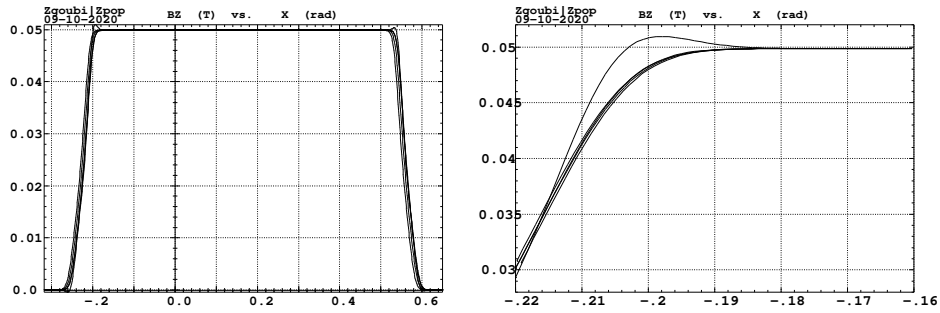


Fig. 17.76 Magnetic field along 5 different trajectories across the upstream DIPOLE, including four large horizontal and vertical excursion cases, and a zoom in on the entrance fringe field region

6309 (d) Sinusoidal approximation of the betatron motion

The approximation

$$y(\theta) = A \cos(\nu_Z \theta + \phi)$$

6310 is checked here considering the vertical motion (considering the horizontal motion
6311 leads to similar conclusions). The value of the various parameters in that expression
6312 are determined as follows:

- the particle raytraced for comparison is launched with an initial excursion $Z_0(\theta = 0) = 5$ cm (4th particle in OBJET, above). At the launch point (middle of the long drift) the beam ellipse is upright (Fig. 17.73), whereas phase space motion is clockwise, thus take

$$A = 5 \text{ cm} \quad \text{and} \quad \phi = \pi/2$$

- the vertical betatron tune of the 4-cell ring is (Tab. 17.65)

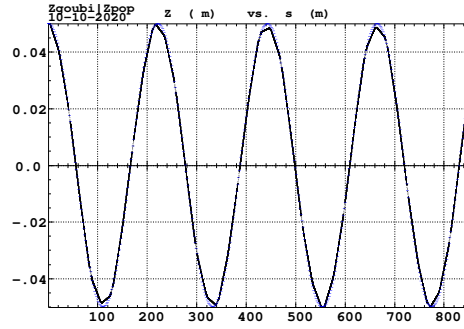
$$\nu_Z = 4 \times 0.192869 = 0.77147$$

- $\theta = s/R$ and $R = \oint ds/2\pi$ with (Tab. 17.65)

$$2\pi R = \text{circumference} = 4 \times 42.72614331 = 170.90457 \text{ m}$$

6313 The comparison with a trajectory obtained from raytracing is given in Fig. 17.77
6314 and confirms the validity of the sinusoidal approximation.

Fig. 17.77 Vertical betatron motion, five turns around the ZGS ring, from raytracing (continuous line), and sine approximation, superimposed (dashed line)



6315 (e) An acceleration cycle. Symplecticity checks.

Eleven particles are launched for 65,000 turn tracking at a rate of

$$\Delta W = q\hat{V} \cos \phi_s = 400 \times \sin 150^\circ = 200 \text{ keV/turn}$$

6316 ($E : 0.05 \rightarrow 13.05 \text{ GeV}$), all evenly distributed on the same initial vertical invariant

$$Z^2/\beta_Z + \beta_Z Z'^2 = \varepsilon_Z/\pi \quad (17.17)$$

6317 with $\varepsilon_Z/\pi = 10^{-4} \text{ m}$, or, normalized, $\beta\gamma\varepsilon_Z/\pi = 0.33078 \times 10^{-4} \text{ m}$.

The simulation file is given in Tab. 17.67. CAVITE[IOPT=3] is used, it provides an RF phase independent boost

$$\Delta W = q\hat{V} \sin \phi_s$$

6318 as including synchrotron motion is not necessary here, even better, this ensures
6319 constant depolarizing resonance crossing speed, so precluding any possibility of
6320 multiple crossing (it can be referred to [3] regarding that effect).

Table 17.67 Simulation input data file: track 11 particles launched on the same vertical invariant, with quasi-zero horizontal invariant. The INCLUDE adds the ZGS cell four times, the latter is defined in Tab. 17.63 and Fig. 9.24. An MCOBJET is commented, it is used in a subsequent spin tracking exercise

```

ZGS ring. Polarization landscape.
'MARKER' ZGSPolarLand_S ! Just for edition purposes.
'OBJET'
1.03527036749193e3 ! Reference Brho: 50 MeV proton.
8 ! Create a 13 particle set, proper for MATRIX computation.
1 11 1 ! Define 9 particles, all with ~0 horiz. invarient, evenly spread on same vertical invariant.
0. 0. 0. 0. 0. 1. 'o' ! Reference trajectory: all initial coordinates nul, relative rigidity D=1.
0. 28.63 0. ! Horiz. invarient taken zero. Nominal would be 0.14mu_m norm. i.e. 4.6e-8 non-normalized.
0. 37.01 150e-6 ! epsilon_Z/pi = beta.gamma * epsilon_norm, latter =0.05e-6 m, beta.gamma=0.3308.
0. 1. 0. 0. ! All paricles are on-momentum.

!'MCOBJET' ! Commented.
!1.03527036749193e3 ! Reference Brho: 50 MeV proton.
!3 ! Create random coordinates.
!200
!2 2 2 2 2
!0. 0. 0. 0. 0. 1.
!0. 28.63 25e-6 3 ! Periodic alpha_Y, beta_Y, and invariant value;
!0. 37.01 10e-6 3 ! Periodic alpha_Z, beta_Z, and invariant value.
!0. 1. 1.e-8 3
!123456 234567 345678

'PARTICUL'
PROTON ! Necessary data in order to allow (i) spin trackingand, and (ii) acceleration.
'SPNTRK' ! Switch on spin tracking,
3 ! all initial spins vertical.
'FAISCEAU'
'FAISTORE'
b_polarLand.fai ! Log particle data in b_polarLand.fai, turn-by-turn; "b_" imposes
7 ! binary write, which results in faster i/o.

'SCALING'
1 1
DIPOLE
-1 ! Causes field increase in DIPOLE, in correlation to particle
1. ! rigidity increase by CAVITE.
1

! 4 cells follow.
'INCLUDE'
1
4* ./ZGS_cell.inc[S_ZGS_cell:E_ZGS_cell]

'CAVITE'
3
0 0
400e3 0.523598775598 ! Acceleration rate is 400*0.5=200keV/turn.

'REBELOTE'
87000 0.3 99

'FAISCEAU'
'MARKER' ZGSPolarLand_E ! Just for edition purposes.
'SPNPRT'

'END'

```

6321 *Betatron damping*

6322 Figure 17.78 shows the damped vertical motion of the individual particles, over
 6323 the acceleration range, together with the initial and final distributions of the 11
 6324 particles on elliptical invariants. Departure from the matching ellipse at the end of
 6325 the acceleration cycle, 13 GeV (Eq. 17.17 with $\varepsilon_Z/\pi = 2.2244 \times 10^{-7}$ m), is marginal.

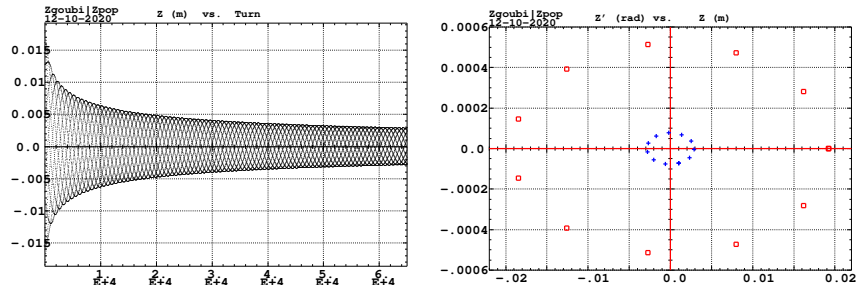
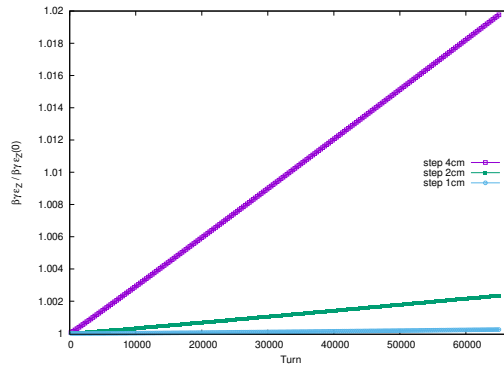


Fig. 17.78 Left: damped vertical motion, from 50 MeV to 13.05 GeV, 65,001 turns. Right: the initial coordinates of the 11 particles (squares) are taken on a common invariant $\epsilon_Z(0) = 10^{-5} \pi \text{ m}$ (at 50 MeV, $\beta\gamma = 0.33078$, thus $\beta\gamma\epsilon_Z(0) = 0.33078 \times 10^{-5} \pi \text{ m}$); the final coordinates after 65,000 turns (crosses) appear to still be (with negligible departure) on a common invariant of value $\epsilon_Z(\text{final}) = 2.2244 \times 10^{-7} \pi \text{ m}$ (at 13 GeV, $\beta\gamma = 14.869842$) thus $\beta\gamma\epsilon_Z(\text{final}) = 0.33076 \times 10^{-5} \pi \text{ m}$, equal to the initial value

6326 *Degree of non-symplecticity of the numerical integration*

6327 The degree of non-symplecticity as a function of integration step size is illustrated
 6328 in Fig. 17.79. The initial motion is taken paraxial, vertical motion is considered as
 6329 it resorts to off-mid plane Taylor expansion of fields [1, DIPOLE Sect.], a stringent
 6330 test as the latter is expected to deteriorate further the non-symplecticity inherent
 6331 to the Lorentz equation integration method (a truncated Taylor series method [1,
 6332 Eq. 1.2.4]).

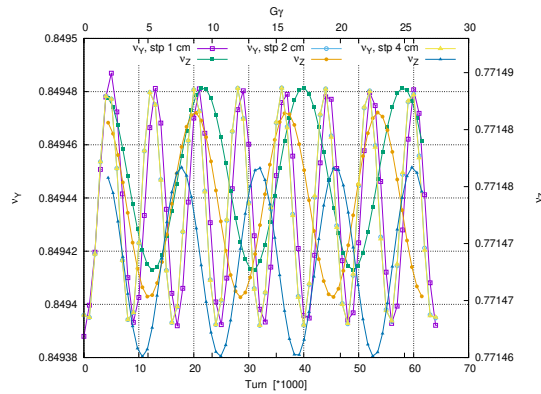
Fig. 17.79 Turn-by-turn evolution of the normalized invariant, $\beta\gamma\epsilon_Z(\text{turn})/\beta\gamma\epsilon_Z(0)$ (initial $\epsilon_Z(0)$ taken paraxial), for four different integration step size values: 1, 2 and 4 cm



6333 *Evolution of the wave numbers.*

6334 The Fortran tool `tunesFromFai_iterate` can be used to compute tunes as a function
 6335 of turn number or energy, it reads turn-by-turn particle data from `zgoubi.fai` and
 6336 computes a discrete Fourier transform over so many turns (a few tens, for instance),
 6337 every so many turns [4]. Typical results are displayed in Fig. 17.80, tunes have the
 6338 expected values: $\nu_Y = 0.849$, $\nu_Z = 0.771$. An acceleration rate of 200 keV/turn has
 6339 been taken (namely, $\hat{V} = 400$ kV and still $\phi_s = 150^\circ$), to save on computing time.
 6340 Note that turn-by-turn raytracing allows determining the tune value at all γ along the
 6341 acceleration cycle (and thus for instance the γ values at which the resonance occurs,
 6342 see (f)). In these simulations anyway the horizontal and vertical tunes are essentially
 6343 constant over the all cycle: it is determined by the wedge angle, which won't change
 6344 as long as the reference orbit isn't changed. The latter holds here, as SCALING with
 6345 option NTIM=-1 causes the magnet field to strictly follow the momentum boost by
 6346 CAVITE.

Fig. 17.80 Horizontal ring tune (left vertical axis), $\nu_Y \approx 0.8494$, and vertical ring tune (right vertical axis), $\nu_Z \approx 0.77147$, as a function of turn number, over 65,000 turns ($E : 0.05 \rightarrow 13$ GeV at a rate of 200 keV/turn). The graph displays results for 3 different integration step sizes, namely, 1, 2 and 4 cm, essentially converged



6347 (f) Crossing an isolated intrinsic depolarizing resonance.

6348 The simulation uses the input data file of Tab. 17.67, with the following changes:

6349 • Under OBJET:

- 6350 – 1st line, change the reference rigidity *BORO* to the proper value, a few thousand turns upstream of the resonance to be crossed,
- 6351 – 3rd line, request a single particle (“1 1 1”, in lieu of “1 11 1”),
- 6352 – 6th line, set the invariant ε_Z/π to the desired value, ε_Y/π value is indifferent;

- 6354 • change the field value under DIPOLE consistently with the new *BORO* value, so to maintain the expected curvature radius $\rho_0 = BORO/B = 20.76$ m (Tab. 9.2,
- 6355 • under CAVITE, provide the desired peak voltage \hat{V} ,
- 6356 • under REBELOTE, set the number of turns: a few thousands of turns upstream and downstream of the resonance.
- 6357
- 6358

6359 On the other hand, similar simulations are performed in questions (f)-(i) of
6360 exercise 9.1. Please refer to the solutions of these SATURNEI simulations.

6361 (g) Study of an imperfection depolarizing resonance.

6362 The simulation data files of question (f) can be used here, *mutatis mutandis*, and
6363 the methodology in (f) can be followed.

6364 On the other hand, similar simulations are performed in questions (f)-(i) of
6365 exercise 9.1, as well as in the “Strong Focusing Synchrotron” Chapter, Sect. 17.5.
6366 Please refer to the solutions of these simulations.

6367 (g) Spin tracking. Bunch polarization.

Spin depolarizing resonances in the ZGS are located at

$$G\gamma_R = kP \pm \nu_Z = 4 - \nu_Z, 4 + \nu_Z, 8 - \nu_Z, 8 + \nu_Z, 12 - \nu_Z, \text{ etc.}$$

6368 with $P=4$ the superperiodicity of the ring, and $\nu_Z = 0.77147$ taken from Tab. 17.65,
6369 or from Fig. 17.80. $G\gamma_R$ is bounded, in the present simulation, by $G\gamma(17.4 \text{ GeV}) =$
6370 $35.0 < 9P - \nu_Z$. Resonances are expected to be stronger at $G\gamma_R = 2 \times 4k \pm \nu_Z =$
6371 $8 - \nu_Z, 8 + \nu_Z, 16 - \nu_Z, \text{ etc.}$, with the additional factor 2 the number of cells per
6372 superperiod [6, Sect. 3.II].

The simulation data file to track through these resonances is the same as in ques-
tion (e), Tab. 17.67, except for the substitution of MCOBJET (to be uncommented) to
OBJET (to be commented). MCOBJET creates a 200 particle bunch with Gaussian
transverse and longitudinal densities, with the following *rms* values at 50 MeV:

$$\varepsilon_Y/\pi = 25 \mu\text{m}, \quad \varepsilon_Z/\pi = 10 \mu\text{m}, \quad \frac{dp}{p} = 10^{-4}$$

6373 which are presumably close to ZGS polarized proton runs [7]. CAVITE accelerates
6374 that bunch from 50 MeV to 17.4 GeV about, at a rate of $q\hat{V} \sin(\phi_s) = 200 \text{ keV/turn}$
6375 ($\hat{V} = 400 \text{ kV}$, $\phi_s = 30^\circ$), in 87,000 turns about.

6376 Figure 17.81 shows sample S_Z spin components of a few particles taken among
6377 the 200 tracked. Figure 17.82 displays $\langle S_Z \rangle$, the vertical polarization component of
6378 the 200 particle set. A gnuplot script is used, given in Tab. 17.68.

Fig. 17.81 Individual vertical spin component of 20 particles accelerated in ZGS from 50 MeV to 17.4 GeV, at a rate of 200 keV/turn. A graph obtained using zpop, data read from [b_]zgoubi.fai; menu 7; 1/2 to open b_zgoubi.fai; 2/[20,23] for S_Z versus turn; 7 to plot

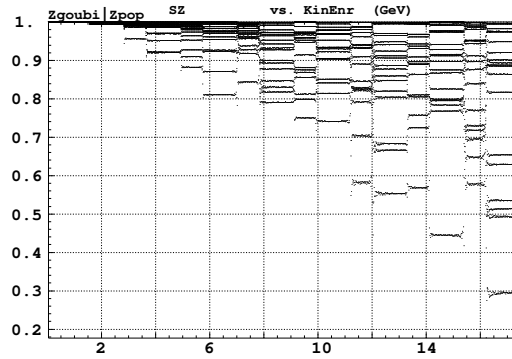


Fig. 17.82 Average vertical component of the polarization vector of a 200 particle bunch, accelerated from 50 MeV to 17.4 GeV. The vertical lines materialize the locations $G\gamma_R = 4k \pm \nu_Z$ of the depolarizing resonances. Resonances are stronger at $G\gamma_R = 8k \pm \nu_Z$ (as labeled)

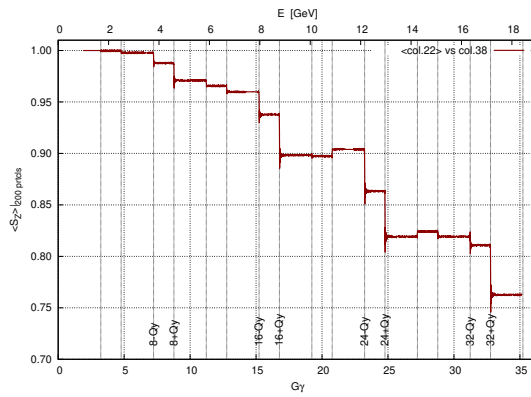


Table 17.68 A gnuplot script to plot the average vertical spin component of the 200 particle set, along the acceleration ramp (Fig. 17.82). The average is prior computed by an awk script, which reads the necessary data from zgoubi.fai.

```
# gnuplot_avrgFromFai.gnu
set x2label "E [GeV]"; set xlabel "G{/Symbol g}"; set ylabel "<S_Z>|_{200 prtcls}"
set xtics nomirror; set x2tics; set ytics; set format y '%0.2f'; set grid
M=938.27208; Ei = 50.; G = 1.79284735; Qy = 0.7715; dE = 0.2 # MeV/turn
fName = 'zgoubi.fai'; plotCmd(col_num)=sprintf('< gawk -f average.awk -v col_num=%d %s', col_num,fName)

do for [integr=1:9] { set arrow nohead from 4*integr+Qy, 0.7 to 4*integr+Qy, 1.01 lw .6 dt 3
set arrow nohead from 4*integr-Qy, 0.7 to 4*integr-Qy, 1.01 lw .6 dt 3 }

do for [integr=8:32:8] { set label " ".integr."-Qy" at integr-Qy, 0.71 rotate by 90
set label " ".integr."+Qy" at integr+Qy, 0.71 rotate by 90 }

set x2r [0:19.]; set xr [0:19000./M*G]; set yr [:-1.01]
plot plotCmd(22) u (G/M*(Ei+($1-1.)*dE +M)):2 w l lw 2 lc rgb 'dark-red' t "<col.22> vs col.38"
```

average.awk script to compute $\langle S_Z \rangle$ [5]:

```
function average(x, data){
  n = 0;mean = 0;
  val_min = 0;val_max = 0;
  for(val in data){
    n += 1;
    delta = val - mean;
    mean += delta/n;
    val_min = (n == 1)?val:((val < val_min)?val:val_min);
    val_max = (n == 1)?val:((val > val_max)?val:val_max);
  }
  if(n > 0){
    print x, mean, val_min, val_max;
  }
}
{
  curr = $38;
  yval = $(col_num);

  if(NR==1 || prev != curr){
    average(prev, data);
    delete data;
    prev = curr; }
  data[yval] = 1; }
END{
  average(curr, data); }
```

References

- 6380 1. Méot, F.: Zgoubi Users' Guide. <https://www.osti.gov/biblio/1062013-zgoubi-users-guide>.
- 6381 Sourceforge latest version: <https://sourceforge.net/p/zgoubi/code/HEAD/tree/trunk/guide/Zgoubi.pdf>.
- 6382 The betaFromPlt.f program is available here: <https://sourceforge.net/p/zgoubi/code/HEAD/tree/trunk/toolbox/betaFromPlt/>
- 6383 2. A postprocessing tool to transport betatron functions step-by-step, using raytracing data stored
- 6384 in zgoubi.plt.
- 6385 <https://sourceforge.net/p/zgoubi/code/HEAD/tree/trunk/toolbox/betaFromPlt/>
- 6386 3. Aniel, T., et al.: Polarized particles at SATURNE. Journal de Physique, Colloque C2, supplée-
- 6387 ment au n02, Tome 46, février 1985, page C2-499.
- 6388 <https://hal.archives-ouvertes.fr/jpa-00224582>
- 6389 4. The Fortran tunesFrmFai_iterate.f, together with a README and an example of its use, can
- 6390 be found at
- 6391 <https://sourceforge.net/p/zgoubi/code/HEAD/tree/trunk/toolbox/tunesFromFai/>
- 6392 5. <https://stackoverflow.com/questions/42677017/plot-average-of-nth-rows-in-gnuplot>
- 6393 6. Lee, S.Y.: Spin Dynamics and Snakes in Synchrotrons. World Scientific, 1997
- 6394 7. Khoe, T.K., et al.: The High Energy Polarized Beam at the ZGS. Procs. IXth Int. Conf on
- 6395 High Energy Accelerators, Dubna, pp. 288-294 (1974)
- 6396 8. Méot, F.: Spinor Methods. In: Polarized Beam Dynamics and Instrumentation in Particle
- 6397 Accelerators, USPAS Summer 2021 Spin Class Lectures, Springer Nature, Open Access (2023).
- 6398 <https://link.springer.com/book/10.1007/978-3-031-16715-7>